arXiv:1605.01279v2 [q-bio.SC] 16 Sep 2016

Uniform asymptotic approximation of diffusion to a small target: generalized reaction models

Samuel A. Isaacson* Ava Mauro† Jay Newby‡

September 19, 2016

Abstract

The diffusion of a reactant to a binding target plays a key role in many biological processes. The reaction-radius at which the reactant and target may interact is often a small parameter relative to the diameter of the domain in which the reactant diffuses. We develop uniform in time asymptotic expansions in the reaction-radius of the full solution to the corresponding diffusion equations for two separate reactant-target interaction mechanisms: the Doi or volume reactivity model, and the Smoluchowski-Collins-Kimball partial absorption surface reactivity model. In the former, the reactant and target react with a fixed probability per unit time when within a specified separation. In the latter, upon reaching a fixed separation, they probabilistically react or the reactant reflects away from the target. Expansions of the solution to each model are constructed by projecting out the contribution of the first eigenvalue and eigenfunction to the solution of the diffusion equation, and then developing matched asymptotic expansions in Laplace-transform space. Our approach offers an equivalent, but alternative, method to the pseudo-potential approach we previously employed in [1] for the simpler Smoluchowski pure absorption reaction mechanism. We find that the resulting asymptotic expansions of the diffusion equation solutions are identical with the exception of one parameter: the diffusion limited reaction rates of the Doi and partial absorption models. This demonstrates that for biological systems in which the reaction-radius is a small parameter, properly calibrated Doi and partial absorption models may be functionally equivalent.

1 Introduction

A variety of bimolecular reaction mechanisms have been used in particle-based stochastic reaction-diffusion models of biological systems. The Doi model assumes two molecules may react with a fixed probability per unit time when their separation is less than some reaction-radius [2, 3, 4]. In the Smoluchowski model molecules either react instantly when their separation equals the

*Department of Mathematics and Statistics, Boston University (isaacson@math.bu.edu)
†Department of Mathematics and Statistics, University of Massachusetts Amherst (mauro@math.umass.edu)
‡Mathematics Department, University of North Carolina, Chapel Hill (jaynewby@email.unc.edu)

reaction-radius (pure absorption reaction) [5], or have a probability of reflection upon collision (Smoluchowski–Collins–Kimball partial absorption reaction) [6].

For each of these reaction models, analytic solutions have been derived and investigated in free space (see the many references in [7]). Inside cells, reactions occur within closed subdomains with complex boundaries. In many such domains the reaction-radius is a small parameter relative to the diameter of the cellular domain. We previously developed a method for calculating uniform in time asymptotic expansions of the solution to the pure absorption Smoluchowski model for diffusion to a fixed target within closed, three-dimensional domains [1]. In this work we extend our previous study to develop uniform in time asymptotic expansions of the solution to the diffusion equation for targets with both Doi and Smoluchowski partial absorption reaction models. Our new results are constructed using matched asymptotic expansions in Laplace-transform space, which offers an equivalent, but alternative, method to the pseudo-potential approach we previously employed. The matched-asymptotics approach has been widely used for related problems that calculate various statistics of first passage times [8, 9, 10, 11, 12]. It is well–suited for handling different reaction models because the solution is constructed from two parts: an inner solution that accounts for behavior near the partially absorbing target while ignoring the detailed shape of the domain boundary, and an outer solution that accounts for the reflecting domain boundary while ignoring the fine-scale details of the target reaction mechanism and surface. As we illustrate in the results section, one benefit to our approach is that the uniform in time expansion of the full diffusion equation we derive can be used to calculate corresponding asymptotic expansions in the reaction-radius of both the first passage time density and moments of the first passage time.

While we focus on the case of a single spherical target in this work, it has been demonstrated that similar expansions of the mean first passage time for a reaction to occur with a target can be extended to problems with multiple, competing reactive targets [9]. We while we do not study the case of multiple targets, we expect our uniform in time expansions of the diffusion equation could be generalized to such problems.

The mathematical problem we consider is diffusion of a molecule within a bounded domain $\Omega \subset \mathbb{R}^3$, containing a small, spherical target, $\Omega_\varepsilon \subset \Omega$, with radius ε centered at $\boldsymbol{r}_\mathrm{b} \in \Omega$. We denote by $\partial\Omega$ the exterior boundary surface to Ω, and by $\partial\Omega_\varepsilon$ the exterior boundary to Ω_ε. The non-target portion of Ω is denoted by $\Omega_{\text{free}} = \Omega \setminus \{\Omega_\varepsilon \cup \partial\Omega_\varepsilon\}$. We assume the molecule moves by Brownian motion within Ω_{free}, with position given by $\boldsymbol{R}(t)$. Denote by $p(\boldsymbol{r}, t)$ the probability density that $\boldsymbol{R}(t) = \boldsymbol{r} \in \Omega_{\text{free}}$, and the molecule has not yet "bound" to the target. Finally, let D label the diffusion constant of the molecule. In this work we consider three distinct models for the binding of the molecule to the target.

The first model is the (pure-absorption) Smoluchowski diffusion limited reaction model [5], where the molecule instantaneously reacts with probability one the moment it reaches the target boundary. In this case $p(\boldsymbol{r}, t)$ satisfies the diffusion equation with a Neumann boundary

condition on the domain boundary,

$$\frac{\partial p}{\partial t} = D\Delta p(\boldsymbol{r},t), \quad \boldsymbol{r} \in \Omega_{\text{free}},\, t > 0, \tag{1.1a}$$

$$\partial_{\boldsymbol{\eta}} p(\boldsymbol{r},t) = 0, \quad \boldsymbol{r} \in \partial\Omega,\, t > 0, \tag{1.1b}$$

with the initial condition $p(\boldsymbol{r},0) = \delta(\boldsymbol{r}-\boldsymbol{r}_0)$ for $\boldsymbol{r}_0 \in \Omega_{\text{free}}$, and the binding reaction modeled by the pure-absorption Dirichlet boundary condition

$$p(\boldsymbol{r},t) = 0, \quad \boldsymbol{r} \in \partial\Omega_\varepsilon,\, t > 0. \tag{1.2}$$

In the preceding equations $\partial_{\boldsymbol{\eta}}$ denotes the directional derivative in the inward normal direction, $\boldsymbol{\eta}(\boldsymbol{r})$, to the boundary at $\boldsymbol{r}$.

A uniform (in time) asymptotic asymptotic expansion of the solution to (1.1) as $\varepsilon \to 0$ has recently been developed by the authors [1]. However, it is often desirable in a given model to include the possibility that the Brownian walker does not instantaneously bind with probability one upon reaching the target, i.e. there is a possibility the walker fails to bind to the target. For example, proteins may have specific binding sites and complex three dimensional shapes that must come together in precise orientations for a reaction to occur. Only a fraction of encounters may then result in a binding event, which is often approximated as a probabilistic event. In this paper we consider two models that allow for the possibility of non-reactive encounters.

The first model replaces the pure-absorption Dirichlet boundary condition (1.2) with a Smoluchowski–Collins–Kimball partial-absorption Robin boundary condition [6],

$$-D\partial_{\boldsymbol{\eta}} p(\boldsymbol{r},t) = \gamma p(\boldsymbol{r},t), \quad \boldsymbol{r} \in \partial\Omega_\varepsilon,\, t > 0. \tag{1.3}$$

Here the Robin constant, γ, determines the intrinsic rate of the reaction [13] when the diffusing molecule is at the surface of the binding region. It typically has units of distance per time. The reactive Robin boundary condition model arises in many ways. For example, it can be interpreted as the limit of a steep potential barrier with small support, which must be surmounted before reaching a pure-absorption reactive boundary [14, 10]. To give a comparable asymptotic expansion of $p(\boldsymbol{r},t)$ as $\varepsilon \to 0$ to that of the pure absorption boundary condition, we assume

$$\gamma = \frac{D\hat{\gamma}}{\varepsilon}, \tag{1.4}$$

where the non-dimensional constant, $\hat{\gamma}$, is independent of ε. We may then rewrite the Robin boundary condition as

$$-\partial_{\boldsymbol{\eta}} p(\boldsymbol{r},t) = \frac{\hat{\gamma}}{\varepsilon} p(\boldsymbol{r},t). \tag{1.5}$$

In the Doi model [2, 3, 15] the reactive boundary conditions of the previous two models are replaced by an effective sink term. That is, (1.1a) is coupled to the PDE

$$\frac{\partial p}{\partial t} = D\Delta p(\boldsymbol{r},t) - \mu p, \quad \boldsymbol{r} \in \Omega_\varepsilon,\, t > 0, \tag{1.6}$$

within Ω_ε through the assumption that p and $\partial_{\boldsymbol{\eta}} p$ are continuous across $\partial\Omega_\varepsilon$. To give a comparable asymptotic limit of $p(\boldsymbol{r}, t)$ as $\varepsilon \to 0$ to those of the reactive boundary condition models (assuming $\boldsymbol{r}$ and $\boldsymbol{r}_0$ are $O(1)$ distance from the target), we assume

$$\mu = \frac{D\hat{\mu}}{\varepsilon^2}, \tag{1.7}$$

where the non-dimensional constant, $\hat{\mu}$, is independent of ε. We note that both scalings (1.4) and (1.7) are necessary for each reaction mechanism to be *partially* absorbing as $\varepsilon \to 0$. Different scaling choices lead either to no absorption (e.g., if the rates are $O(1)$) or perfect absorption, which is equivalent to the pure absorption Smoluchowski model. Using (1.7), we may rewrite (1.6) as

$$\frac{\partial p}{\partial t} = D\Delta p(\boldsymbol{r}, t) - \frac{D\hat{\mu}}{\varepsilon^2} p, \quad \boldsymbol{r} \in \Omega_\varepsilon,\ t > 0. \tag{1.8}$$

The paper is organized as follows. First, we develop the uniform asymptotic approximation in Section 2. A new feature of this work is the use of matched asymptotic expansions in Laplace-transform space to develop the "short-time" component of the asymptotic expansion. This component corresponds to the solution of (1.1) with one of the reactive mechanisms (1.2), (1.5) or (1.8), but with the first eigenfunction contribution to the initial condition projected out. In Ref. [1] we developed this expansion for the pure-absorption boundary condition (1.2) by replacing the boundary condition with an appropriately calibrated pseudo-potential operator and a subsequent perturbation expansion of the new PDE. In this paper, we develop expansions that establish the equivalence of the pseudo-potential approach to matched asymptotic expansions in Laplace-transform space through terms of $O(\varepsilon^2)$. We find that when the diffusion limited reaction rates of the partial absorption (1.5) and Doi (1.8) reaction models are calibrated to be the same, the resulting outer expansions of the solutions to the corresponding diffusion equations, and hence also outer expansions of any first passage time statistics, are identical.

Finally, in Section 3 we show results for a spherical domain. We compare the asymptotic approximation of $p(\boldsymbol{r}, t)$ to the exact solution of the spherically symmetric problem (i.e. when the target is at the center and the initial position is uniformly distributed over the sphere of radius r_0), and to Monte Carlo simulations when the target is not centered. These results demonstrate that our asymptotic expansions are able to capture short time effects, including multimodality in the first passage time density, which are not present in long time expansions (where the first passage time density is approximated as exponential).

2 Uniform asymptotic approximation

Let $-\lambda$ denote the principal, e.g. smallest magnitude, eigenvalue of the generator for the diffusion problem (1.1a) with reaction mechanism (1.2), (1.5) or (1.8). That is, λ is the principal eigenvalue of the Laplacian operator, $-\Delta$, with the boundary condition (1.1b) and the reactive

boundary condition (1.2) for the pure absorption Smoluchowski model, or the reactive boundary condition (1.5) for the partial absorption Smoluchowski–Collins–Kimball model. In the Doi model the generator is the operator

$$-\Delta + \frac{\hat{\mu}}{\varepsilon^2}\mathbb{1}_{[0,\varepsilon]}(\boldsymbol{r})$$

with the boundary condition (1.1b). Here $\mathbb{1}_{\Omega_\varepsilon}(\boldsymbol{r})$ denotes the indicator function of Ω_ε.

Our basic approach is to first split $p(\boldsymbol{r},t)$ into two components: a large time approximation that will accurately describe the behavior of $p(\boldsymbol{r},t)$ for $\lambda Dt \gg 1$, and a short time correction to this approximation when $\lambda Dt \not\gg 1$. Note, both are defined for all times, but the latter approaches zero as $t \to \infty$, and so only provides a significant contribution for $\lambda Dt \not\gg 1$. It should be stressed that the short time correction is not an asymptotic approximation of $p(\boldsymbol{r},t)$ as $t \to 0$, but instead serves as a correction to the long time expansion for $\lambda Dt \not\gg 1$. We write $p(\boldsymbol{r},t)$ as

$$p(\boldsymbol{r},t) = p_{\text{LT}}(\boldsymbol{r},t) + p_{\text{ST}}(\boldsymbol{r},t), \tag{2.1}$$

where p_{LT} is the "large time" approximation and p_{ST} is the "short time" correction.

We define the large time approximation and short time correction through an eigenfunction expansion of $p(\boldsymbol{r},t)$. Assume the existence of an orthonormal L^2 basis of eigenfunctions for the generator. Let ψ_j label the eigenfunctions and λ_j the eigenvalues, and consider the eigenfunction expansion

$$p(\boldsymbol{r},t) = \sum_{j=0}^{\infty} c_j \psi_j(\boldsymbol{r}) e^{-\lambda_j Dt},$$

where

$$c_j = \int_{\Omega'} p(\boldsymbol{r},0)\psi_j(\boldsymbol{r})d\boldsymbol{r}.$$

Here Ω' denotes the portion of Ω in which the free reactant can diffuse. For the pure and partial absorption models $\Omega' = \Omega_{\text{free}}$, while in the Doi model $\Omega' = \Omega$. With $p(\boldsymbol{r},0) = \delta(\boldsymbol{r}-\boldsymbol{r}_0)$, we obtain

$$p(\boldsymbol{r},t) = \sum_{j=0}^{\infty} \psi_j(\boldsymbol{r}_0)\psi_j(\boldsymbol{r}) e^{-\lambda_j Dt}.$$

For simplicity, in the remainder we denote the principal eigenfunction and corresponding eigenvalue as $\psi(\boldsymbol{r}) := \psi_0(\boldsymbol{r})$ and $\lambda := \lambda_0$.

We will choose the long time approximation to correspond to the first mode of the eigenfunction expansion of $p(\boldsymbol{r},t)$, that is

$$p_{\text{LT}}(\boldsymbol{r},t) := \psi(\boldsymbol{r})\psi(\boldsymbol{r}_0)e^{-\lambda Dt}. \tag{2.2}$$

With this choice, p_{LT} and p_{ST} satisfy the projected initial conditions

$$p_{\text{LT}}(\boldsymbol{r},0) = \langle \psi(\boldsymbol{r}), \delta(\boldsymbol{r}-\boldsymbol{r}_0)\rangle\, \psi(\boldsymbol{r}), \tag{2.3}$$

$$p_{\text{ST}}(\boldsymbol{r},0) = \delta(\boldsymbol{r}-\boldsymbol{r}_0) - \psi(\boldsymbol{r})\psi(\boldsymbol{r}_0), \tag{2.4}$$

where $\langle \cdot, \cdot \rangle$ denotes the L^2 inner product,

$$\langle u(\boldsymbol{r}), w(\boldsymbol{r}) \rangle = \int_{\Omega'} u(\boldsymbol{r}) w(\boldsymbol{r}) d\boldsymbol{r}.$$

By adding the two solutions, we see that the original initial condition is satisfied.

In [1] we used this splitting to aid in determining uniform in time asymptotic expansions of the solution to the pure-absorption Dirichlet problem. One benefit to this approach is that the long time approximation of the Dirichlet, Robin and Doi problems can be obtained by adapting the matched asymptotics method developed in [8, 9].

In the remainder of this section, we show using the method of matched asymptotics that the short- and long-time parts of the uniform outer expansions as $\varepsilon \to 0$ of the Dirichlet, Robin and Doi problems are identical in form. We find that they differ by only a single parameter: the diffusion limited reaction rate.

In some applications, the detailed spatial dynamics within each of the preceding models can be ignored, and the reactive process can be characterized as a well-mixed bimolecular reaction with rate constant given by this diffusion limited rate. For the pure-absorption reactive boundary condition, Smoluchowski developed a popular method for deriving the diffusion limited rate (for reactions in an unbounded domain) as function of the microscopic parameters of the preceding models [5]. Denote by k_{S} the diffusion limited rate. Smoluchowski obtained that $k_{\mathrm{S}} = \hat{k}_{\mathrm{S}}\varepsilon$, where

$$\hat{k}_{\mathrm{S}} = 4\pi D. \tag{2.5}$$

Similar expressions have been derived for the Robin boundary condition reaction model [13], where $k_{\mathrm{R}} = \hat{k}_{\mathrm{R}}\varepsilon$ with

$$\hat{k}_{\mathrm{R}} = \frac{4\pi D\hat{\gamma}}{1+\hat{\gamma}}. \tag{2.6}$$

A diffusion limited reaction rate for the Doi reaction mechanism (1.8) was derived in [16], $k_{\mathrm{D}} = \hat{k}_{\mathrm{D}}\varepsilon$ with

$$\hat{k}_{\mathrm{D}} = 4\pi D\left(1 - \frac{\tanh\left(\sqrt{\hat{\mu}}\right)}{\sqrt{\hat{\mu}}}\right). \tag{2.7}$$

Note, in the limit that $\hat{\gamma} \to \infty$, $k_{\mathrm{R}} \to k_{\mathrm{S}}$ [13]. Similarly, as $\hat{\mu} \to \infty$, $k_{\mathrm{D}} \to k_{\mathrm{S}}$ [15]. The pure-absorption reaction model may therefore be interpreted as a limiting case of the partial-absorption and Doi reaction models.

2.1 $\varepsilon = 0$ solutions

We will find it convenient to represent the desired asymptotic expansions in terms of solutions to both time-dependent and stationary $\varepsilon = 0$ problems. We denote by $G(\boldsymbol{r}, \boldsymbol{r}', t)$ the solution of

the $\varepsilon = 0$ limit of (1.1), i.e. the Green's function satisfying

$$\begin{aligned} \frac{\partial G}{\partial t}(\boldsymbol{r}, \boldsymbol{r}', t) &= D\Delta G, \quad \boldsymbol{r} \in \Omega,\, t > 0, \\ \partial_{\boldsymbol{\eta}} G(\boldsymbol{r}, \boldsymbol{r}', t) &= 0, \quad \boldsymbol{r} \in \partial\Omega,\, t > 0, \\ G(\boldsymbol{r}, \boldsymbol{r}', 0) &= \delta(\boldsymbol{r} - \boldsymbol{r}'). \end{aligned} \tag{2.8}$$

In later calculations we will often write G in terms of a part that is regular (bounded) as $t \to 0$ for all $\boldsymbol{r}$ and $\boldsymbol{r}'$, $R(\boldsymbol{r}, \boldsymbol{r}', t)$, and a corresponding singular part (the freespace Green's function with delta function initial condition),

$$G(\boldsymbol{r}, \boldsymbol{r}', t) = R(\boldsymbol{r}, \boldsymbol{r}', t) + \frac{1}{(4\pi D t)^{3/2}} e^{-|\boldsymbol{r}-\boldsymbol{r}'|^2/4Dt}.$$

We will also make use of the unique Neumann function, or pseudo-Green's function, denoted by $U(\boldsymbol{r}, \boldsymbol{r}')$ and satisfying

$$\begin{aligned} -D\Delta_{\boldsymbol{r}} U(\boldsymbol{r}, \boldsymbol{r}') &= -\frac{1}{|\Omega|} + \delta(\boldsymbol{r} - \boldsymbol{r}'), \quad \boldsymbol{r} \in \Omega, \\ \partial_{\boldsymbol{\eta}} U(\boldsymbol{r}, \boldsymbol{r}') &= 0, \qquad\qquad\qquad\quad \boldsymbol{r} \in \partial\Omega, \\ \int_\Omega U(\boldsymbol{r}, \boldsymbol{r}')\, d\boldsymbol{r} &= 0. \end{aligned} \tag{2.9}$$

We similarly split $U(\boldsymbol{r}, \boldsymbol{r}')$ into a part that is regular for all $\boldsymbol{r}$ and $\boldsymbol{r}'$, $R_0(\boldsymbol{r}, \boldsymbol{r}')$, and a singular part as $\boldsymbol{r} \to \boldsymbol{r}'$,

$$U(\boldsymbol{r}, \boldsymbol{r}') = R_0(\boldsymbol{r}, \boldsymbol{r}') + \frac{1}{\hat{k}_S\, |\boldsymbol{r} - \boldsymbol{r}'|}, \tag{2.10}$$

see [11].

We subsequently denote the Laplace transform of a function, $f(t)$, by

$$\mathcal{L}[f](s) = \tilde{f}(s) := \int_0^\infty f(t) e^{-st}\, dt,$$

so that

$$\tilde{G}(\boldsymbol{r}, \boldsymbol{r}', s) = \tilde{R}(\boldsymbol{r}, \boldsymbol{r}', s) + \frac{e^{-|\boldsymbol{r}-\boldsymbol{r}'|\sqrt{\frac{s}{D}}}}{\hat{k}_S\, |\boldsymbol{r} - \boldsymbol{r}'|}.$$

In what follows we will make use of the basic identities

$$\begin{aligned} \lim_{s\to 0} \mathcal{L}\left[G(\boldsymbol{r}, \boldsymbol{r}', t) - \frac{1}{|\Omega|}\right] &= \int_0^\infty \left(G(\boldsymbol{r}, \boldsymbol{r}', t) - \frac{1}{|\Omega|}\right) dt = U(\boldsymbol{r}, \boldsymbol{r}'), \\ \lim_{s\to 0} \mathcal{L}\left[R(\boldsymbol{r}, \boldsymbol{r}', t) - \frac{1}{|\Omega|}\right] &= \int_0^\infty \left(R(\boldsymbol{r}, \boldsymbol{r}', t) - \frac{1}{|\Omega|}\right) dt = R_0(\boldsymbol{r}, \boldsymbol{r}'), \\ \int_0^\infty \frac{1}{(4\pi D t)^{3/2}} e^{-|\boldsymbol{r}-\boldsymbol{r}'|^2/4Dt}\, dt &= \frac{1}{\hat{k}_S\, |\boldsymbol{r} - \boldsymbol{r}'|}. \end{aligned} \tag{2.11}$$

The first identity follows by replacing $G(\boldsymbol{r},\boldsymbol{r}',t)$ by $G(\boldsymbol{r},\boldsymbol{r}',t)-|\Omega|^{-1}$ in (2.8), and integrating in time. The second follows by applying the first and third identities to the representations of $G(\boldsymbol{r},\boldsymbol{r}',t)$ and $U(\boldsymbol{r},\boldsymbol{r}')$ in terms of smooth and singular parts. For readers interested in more detailed derivations of the first two identities see [11, 1].

2.2 Large time component asymptotic expansion

From the eigenfunction expansion of $p(\boldsymbol{r},t)$, in each model we expect for long times that the solution, $p(\boldsymbol{r},t)$, to (1.1a), should be well-approximated by the corresponding first term in the eigenfunction expansion,

$$p(\boldsymbol{r},t) \sim p_{\text{LT}}(\boldsymbol{r},t) = \psi(\boldsymbol{r})\psi(\boldsymbol{r}_0)e^{-\lambda Dt}, \quad t\to\infty.$$

In this section we apply the matched asymptotics approach developed in [8, 11] for calculating asymptotic expansions as $\varepsilon\to 0$ of $\psi(\boldsymbol{r})$ and λ in the pure-absorption Smoluchowski model to the Robin boundary condition and Doi reactive sink models. We derive analogous expansions for the latter two models to those presented in [11, 1] for the pure-absorption Smoluchowski model. Note, a number of results regarding the leading order term for the Robin problem were previously derived in [8], and can be extended to give the inner solution we obtain, (2.20), using the capacitance for the Robin problem derived in [8] within the expansions of [11].

The principal eigenfunction and eigenvalue satisfy

$$\begin{aligned} -\Delta\psi(\boldsymbol{r}) &= \lambda\psi(\boldsymbol{r}), \quad \boldsymbol{r}\in\Omega_{\text{free}},\\ \partial_{\boldsymbol{\eta}}\psi(\boldsymbol{r}) &= 0, \qquad\quad \boldsymbol{r}\in\partial\Omega,\\ \int_{\Omega_{\text{free}}} |\psi(\boldsymbol{r})|^2\,d\boldsymbol{r} &= 1, \end{aligned}$$

with the reactive boundary condition

$$-\partial_{\boldsymbol{\eta}}\psi(\boldsymbol{r}) = \frac{\hat{\gamma}}{\varepsilon}\psi(\boldsymbol{r}), \quad \boldsymbol{r}\in\partial\Omega_\varepsilon, \tag{2.12}$$

in the Robin model, and the reactive sink term

$$-\Delta\psi(\boldsymbol{r}) + \frac{\hat{\mu}}{\varepsilon^2}\psi(\boldsymbol{r}) = \lambda\psi(\boldsymbol{r}), \quad \boldsymbol{r}\in\Omega_\varepsilon, \tag{2.13}$$

in the Doi model (coupled with continuity of $\psi(\boldsymbol{r})$ and $\partial_{\boldsymbol{\eta}}\psi(\boldsymbol{r})$ across $\partial\Omega_\varepsilon$). We assume the eigenfunction is normalized in $L^2(\Omega_{\text{free}})$ (resp. $L^2(\Omega)$) for the Smoluchowski and Robin (resp. Doi) models.

For each model we seek an expansion,

$$\psi(\boldsymbol{r}) \sim \frac{1}{\sqrt{|\Omega|}} + \varepsilon\,\psi^{(1)}(\boldsymbol{r}) + \varepsilon^2\,\psi^{(2)}(\boldsymbol{r}), \quad \varepsilon\to 0, \tag{2.14}$$

where the leading order term is given by the principal eigenfunction of the $\varepsilon = 0$ problem (*i.e.* the principal eigenfunction of $-\Delta$ on Ω with zero Neumann boundary conditions on $\partial\Omega$). Similarly, we seek a corresponding expansion of the principal eigenvalue,

$$\lambda \sim \varepsilon\,\lambda^{(1)} + \varepsilon^2\,\lambda^{(2)}, \quad \varepsilon \to 0. \tag{2.15}$$

Since the principal eigenvalue of $-\Delta$ with zero Neumann boundary conditions on $\partial\Omega_\varepsilon$ is zero, the leading order expansion of λ will be $O(\varepsilon)$ [11, 1].

Following [11] we construct an outer expansion of the principal eigenfunction with the form (2.14), and a corresponding inner expansion of $\psi(\boldsymbol{r})$ near the target, denoted by ϕ. We assume $\psi^{(0)}(\boldsymbol{r}) = |\Omega|^{-1/2}$, consistent with the limit of $\psi(\boldsymbol{r})$ as $\varepsilon \to 0$. To derive an expansion of ϕ, we change to a coordinate system near the reactive boundary/region

$$\boldsymbol{y} = \frac{\boldsymbol{r} - \boldsymbol{r}_\mathrm{b}}{\varepsilon},$$

giving the inner problem

$$-\Delta_{\boldsymbol{y}}\phi(\boldsymbol{y}) = \varepsilon^2\lambda\phi(\boldsymbol{y}), \quad |\boldsymbol{y}| > 1, \tag{2.16}$$

with $\phi(\boldsymbol{y})$ satisfying either the reactive Robin boundary condition

$$-\partial_{\boldsymbol{\eta}}\phi(\boldsymbol{y}) = \hat{\gamma}\phi(\boldsymbol{y}), \quad |\boldsymbol{y}| = 1, \tag{2.17}$$

on the unit sphere, or satisfying the eigenvalue equation with a reactive sink inside the unit sphere,

$$-\Delta_{\boldsymbol{y}}\phi(\boldsymbol{y}) + \hat{\mu}\phi(\boldsymbol{y}) = \varepsilon^2\lambda\phi(\boldsymbol{y}), \quad |\boldsymbol{y}| < 1$$

(with continuity of $\phi(\boldsymbol{y})$ and $\partial_{\boldsymbol{\eta}}\phi(\boldsymbol{y})$ across the unit sphere). We then consider the expansion

$$\phi(\boldsymbol{y}) \sim \phi^{(0)}(\boldsymbol{y}) + \varepsilon\phi^{(1)}(\boldsymbol{y}) + \varepsilon^2\phi^{(2)}(\boldsymbol{y}), \quad \varepsilon \to 0.$$

Substitution into (2.16) gives

$$-\Delta_{\boldsymbol{y}}\phi^{(i)}(\boldsymbol{y}) = 0, \quad |\boldsymbol{y}| > 1, \tag{2.18}$$

with the reactive boundary condition (2.17) for each $\phi^{(i)}$, or the reactive sink equation within the unit sphere

$$-\Delta_{\boldsymbol{y}}\phi^{(i)}(\boldsymbol{y}) + \hat{\mu}\phi^{(i)}(\boldsymbol{y}) = 0, \quad |\boldsymbol{y}| < 1. \tag{2.19}$$

Let $\phi^{(i)}_\infty = \lim_{|\boldsymbol{y}|\to\infty}\phi^{(i)}(\boldsymbol{y})$. The solution to (2.18) with the reactive boundary condition (2.17) is then

$$\phi^{(i)}_\mathrm{R}(\boldsymbol{y}) = \phi^{(i)}_{\mathrm{R},\infty}\left[1 - \frac{\hat{k}_\mathrm{R}}{4\pi D}\frac{1}{|\boldsymbol{y}|}\right], \quad |\boldsymbol{y}| > 1, \tag{2.20}$$

where $\hat{k}_{\mathrm{R}}$ is given by (2.6). The corresponding solution to (2.18) with the Doi reaction model (2.19) is then

$$\phi_{\mathrm{D}}^{(i)}(\boldsymbol{y}) = \begin{cases} \phi_{\mathrm{D},\infty}^{(i)} \left(1 - \frac{\hat{k}_{\mathrm{D}}}{4\pi D}\right) \frac{\sinh\left(\sqrt{\hat{\mu}}\,|\boldsymbol{y}|\right)}{\sinh\left(\sqrt{\hat{\mu}}\right)|\boldsymbol{y}|}, & |\boldsymbol{y}| < 1, \\ \phi_{\mathrm{D},\infty}^{(i)} \left[1 - \frac{\hat{k}_{\mathrm{D}}}{4\pi D} \frac{1}{|\boldsymbol{y}|}\right], & |\boldsymbol{y}| > 1, \end{cases} \tag{2.21}$$

where $\hat{k}_{\mathrm{D}}$ is given by (2.7).

Notice, for $|\boldsymbol{y}| > 1$, the terms of the inner expansion for each of the two models differ only in the diffusion limited rate that appears. This also holds for the pure-absorption Smoluchowski model [11, 1], and as such we subsequently consider

$$\phi^{(i)}(\boldsymbol{y}) = \phi_{\infty}^{(i)} \left[1 - \frac{\hat{k}}{4\pi D} \frac{1}{|\boldsymbol{y}|}\right], \quad |\boldsymbol{y}| > 1,$$

where $\hat{k} \in \{\hat{k}_{\mathrm{S}}, \hat{k}_{\mathrm{R}}, \hat{k}_{\mathrm{D}}\}$ and $\phi_{\infty}^{(i)} \in \{\phi_{\mathrm{S},\infty}^{(i)}, \phi_{\mathrm{R},\infty}^{(i)}, \phi_{\mathrm{D},\infty}^{(i)}\}$ as appropriate for each model.

We now develop the asymptotic expansion of the outer solution. From the perspective of the outer solution, the reactive surface/region simply corresponds to the point, $\boldsymbol{r}_{\mathrm{b}}$. As such, we find upon substitution of the expansions (2.15) and (2.14) that

$$-\Delta\psi^{(i)}(\boldsymbol{r}) = \sum_{j=1}^{i} \lambda^{(j)} \psi^{(i-j)}(\boldsymbol{r}), \quad \boldsymbol{r} \in \Omega \setminus \{\boldsymbol{r}_{\mathrm{b}}\},\ i \geq 1,$$

with $\partial_{\boldsymbol{\eta}} \psi^{(i)}(\boldsymbol{r}) = 0$ on $\partial\Omega$. The assumption that $\psi(\boldsymbol{r})$ is normalized in the two-norm implies that

$$\int_{\Omega} \psi^{(1)}(\boldsymbol{r})\, d\boldsymbol{r} = 0, \tag{2.22}$$

$$\int_{\Omega} \psi^{(2)}(\boldsymbol{r})\, d\boldsymbol{r} = -\frac{\sqrt{|\Omega|}}{2} \int_{\Omega} \left|\psi^{(1)}(\boldsymbol{r})\right|^2 d\boldsymbol{r}. \tag{2.23}$$

To determine the unknown constants, $\phi_{\infty}^{(i)}$, the expansion of λ, and the outer expansion of the principal eigenfunction, $\psi(\boldsymbol{r})$, we match the behavior of the expansion of $\phi(\boldsymbol{y})$ as $|\boldsymbol{y}| \to \infty$ to the behavior of the expansion $\psi(\boldsymbol{r})$ as $\boldsymbol{r} \to \boldsymbol{r}_{\mathrm{b}}$. We note the determination of these expansions is identical to the pure-absorption Dirichlet boundary condition considered in [11], with the only change in the final expansions a modified $\hat{k}$ for the Robin and Doi models. For completeness we now summarize this procedure, but refer the interested reader to [11] for complete details of the derivation, and our previous work [1] for a summary of the final expansions for the pure-absorption reaction mechanism.

At zeroth order we first match $\phi^{(0)}(\boldsymbol{y})$ as $|\boldsymbol{y}| \to \infty$ to $\psi^{(0)}(\boldsymbol{r})$ as $\boldsymbol{r} \to 0$. In the original coordinates we find

$$\phi^{(0)}(\boldsymbol{r}) = \frac{1}{\sqrt{|\Omega|}} \left[1 - \frac{\hat{k}}{4\pi D} \frac{\varepsilon}{|\boldsymbol{r} - \boldsymbol{r}_{\mathrm{b}}|}\right], \quad |\boldsymbol{r} - \boldsymbol{r}_{\mathrm{b}}| > \varepsilon.$$

$\phi^{(0)}(\boldsymbol{r})$ then determines the singular behavior of $\psi^{(1)}(\boldsymbol{r})$ as $\boldsymbol{r} \to \boldsymbol{r}_\mathrm{b}$,

$$\psi^{(1)}(\boldsymbol{r}) \sim -\frac{1}{\sqrt{|\Omega|}} \frac{\hat{k}}{4\pi D} \frac{1}{|\boldsymbol{r} - \boldsymbol{r}_\mathrm{b}|}, \quad \boldsymbol{r} \to \boldsymbol{r}_\mathrm{b}.$$

We therefore find that

$$\begin{aligned} -\Delta\psi^{(1)}(\boldsymbol{r}) &= \frac{\lambda^{(1)}}{\sqrt{|\Omega|}} - \frac{\hat{k}}{D\sqrt{|\Omega|}}\delta(\boldsymbol{r} - \boldsymbol{r}_\mathrm{b}), \quad \boldsymbol{r} \in \Omega, \\ \partial_{\boldsymbol{\eta}}\psi^{(1)}(\boldsymbol{r}) &= 0, \qquad\qquad\qquad\qquad\qquad\quad \boldsymbol{r} \in \partial\Omega, \end{aligned} \tag{2.24}$$

with the normalization condition (2.22). Integrating this equation over Ω and applying the divergence theorem on the left side then gives

$$\lambda^{(1)} = \frac{\hat{k}}{D\,|\Omega|}.$$

Using the Neumann function, $U(\boldsymbol{r}, \boldsymbol{r}_\mathrm{b})$, we may solve (2.24) to find

$$\psi^{(1)}(\boldsymbol{r}) = -\frac{\hat{k}}{\sqrt{|\Omega|}} U(\boldsymbol{r}, \boldsymbol{r}_\mathrm{b}).$$

Matching the regular part of $\psi^{(1)}(\boldsymbol{r})$ as $\boldsymbol{r} \to \boldsymbol{r}_\mathrm{b}$ with the behavior of $\phi^{(1)}(\boldsymbol{y})$ as $\boldsymbol{y} \to \infty$, we find,

$$\phi^{(1)}(\boldsymbol{r}) = \frac{-\hat{k}}{\sqrt{|\Omega|}} R_0(\boldsymbol{r}_\mathrm{b}, \boldsymbol{r}_\mathrm{b}) \left[1 - \frac{\hat{k}}{4\pi D} \frac{\varepsilon}{|\boldsymbol{r} - \boldsymbol{r}_\mathrm{b}|}\right], \quad |\boldsymbol{r} - \boldsymbol{r}_\mathrm{b}| > \varepsilon.$$

$\psi^{(2)}(\boldsymbol{r})$ then has the singular behavior

$$\psi^{(2)}(\boldsymbol{r}) \sim \frac{\hat{k}^2}{4\pi D\sqrt{|\Omega|}} \frac{R_0(\boldsymbol{r}_\mathrm{b}, \boldsymbol{r}_\mathrm{b})}{|\boldsymbol{r} - \boldsymbol{r}_\mathrm{b}|},$$

so that

$$\begin{aligned} -\Delta\psi^{(2)}(\boldsymbol{r}) &= \frac{\lambda^{(2)}}{\sqrt{|\Omega|}} + \lambda^{(1)}\psi^{(1)}(\boldsymbol{r}) + \frac{\hat{k}^2}{D\sqrt{|\Omega|}} R_0(\boldsymbol{r}_\mathrm{b}, \boldsymbol{r}_\mathrm{b})\delta(\boldsymbol{r} - \boldsymbol{r}_\mathrm{b}), \qquad \boldsymbol{r} \in \Omega, \\ \partial_{\boldsymbol{\eta}}\psi^{(2)}(\boldsymbol{r}) &= 0, \qquad\qquad\qquad\qquad\qquad\qquad\qquad\qquad\qquad\quad \boldsymbol{r} \in \partial\Omega, \end{aligned}$$

with the normalization condition (2.23). Integrating over Ω and applying the divergence theorem gives

$$\lambda^{(2)} = -\frac{\hat{k}^2}{D\,|\Omega|} R_0(\boldsymbol{r}_\mathrm{b}, \boldsymbol{r}_\mathrm{b}),$$

so that

$$\psi^{(2)}(\boldsymbol{r}) = \frac{\hat{k}^2}{\sqrt{|\Omega|}}\left[R_0(\boldsymbol{r}_\mathrm{b},\boldsymbol{r}_\mathrm{b})U(\boldsymbol{r},\boldsymbol{r}_\mathrm{b}) - \frac{1}{|\Omega|}\int_\Omega U(\boldsymbol{r},\boldsymbol{r}')U(\boldsymbol{r}',\boldsymbol{r}_\mathrm{b})\,d\boldsymbol{r}'\right] + \bar{\Psi}.$$

Here $\bar{\Psi}$ denotes the average of $\psi^{(2)}$ over Ω, and using (2.23) is given by

$$\bar{\Psi} = -\frac{\hat{k}^2}{2\,|\Omega|^{3/2}}\int_\Omega |U(\boldsymbol{r},\boldsymbol{r}_\mathrm{b})|^2\,d\boldsymbol{r}.$$

In summary, we find

Principal Result 2.1. *The asymptotic outer expansions of the principal eigenfunction and eigenvalue are*

$$\psi(\boldsymbol{r}) \sim \frac{1}{\sqrt{|\Omega|}}\left[1 - \varepsilon\hat{k}U(\boldsymbol{r},\boldsymbol{r}_\mathrm{b}) - \varepsilon^2\hat{k}^2\left(-R_0(\boldsymbol{r}_\mathrm{b},\boldsymbol{r}_\mathrm{b})U(\boldsymbol{r},\boldsymbol{r}_\mathrm{b}) + \frac{1}{|\Omega|}\int_\Omega U(\boldsymbol{r},\boldsymbol{r}')U(\boldsymbol{r}',\boldsymbol{r}_\mathrm{b})\,d\boldsymbol{r}'\right)\right] + \varepsilon^2\bar{\Psi}, \tag{2.25}$$

$$\lambda \sim \lambda_{LT} := \frac{\hat{k}}{D\,|\Omega|}(1 - \hat{k}R_0(\boldsymbol{r}_\mathrm{b},\boldsymbol{r}_\mathrm{b})\varepsilon)\varepsilon, \tag{2.26}$$

with $\hat{k} \in \{\hat{k}_S, \hat{k}_R, \hat{k}_D\}$ as appropriate. Substitution into (2.2) *gives the uniform in time asymptotic expansion of $p_{LT}(\boldsymbol{r},t)$, as given by equations 2.14–2.16 of [1]. Defining*

$$p_{LT}^{(1)}(\boldsymbol{r},\boldsymbol{r}_0,0) = -\frac{\hat{k}}{|\Omega|}\Big(U(\boldsymbol{r},\boldsymbol{r}_\mathrm{b}) + U(\boldsymbol{r}_0,\boldsymbol{r}_\mathrm{b})\Big), \tag{2.27}$$

$$p_{LT}^{(2)}(\boldsymbol{r},\boldsymbol{r}_0,0) = \frac{\hat{k}^2}{|\Omega|}U(\boldsymbol{r},\boldsymbol{r}_\mathrm{b})U(\boldsymbol{r}_0,\boldsymbol{r}_\mathrm{b}) + \frac{\hat{k}^2R(\boldsymbol{r}_\mathrm{b},\boldsymbol{r}_\mathrm{b})}{|\Omega|}\left[U(\boldsymbol{r},\boldsymbol{r}_\mathrm{b}) + U(\boldsymbol{r}_0,\boldsymbol{r}_\mathrm{b})\right] - \frac{\hat{k}^2}{|\Omega|^2}\int_\Omega\left[U(\boldsymbol{r},\boldsymbol{r}') + U(\boldsymbol{r}_0,\boldsymbol{r}')\right]U(\boldsymbol{r}',\boldsymbol{r}_\mathrm{b})\,d\boldsymbol{r}' + \frac{2\bar{\Psi}}{\sqrt{|\Omega|}}, \tag{2.28}$$

we find the small ε expansion of $p_{LT}(\boldsymbol{r},t)$ is then

$$p_{LT}(\boldsymbol{r},t) \sim \left[\frac{1}{|\Omega|} + p_{LT}^{(1)}(\boldsymbol{r},\boldsymbol{r}_0,0)\,\varepsilon + p_{LT}^{(2)}(\boldsymbol{r},\boldsymbol{r}_0,0)\,\varepsilon^2\right]e^{-\lambda_{LT}Dt}. \tag{2.29}$$

2.3 Short time component asymptotic expansion

We now develop an asymptotic expansion as $\varepsilon \to 0$ of $p_{ST}(\boldsymbol{r},t)$, satisfying (1.1) with the projected initial condition (2.4), and one of the reactive models (1.2),(1.5), or (1.8). Our approach differs

from the methods we developed for the pure-absorption Dirichlet problem (1.2) in [1]. There we replaced the reactive boundary condition with a pseudo-potential operator in the underlying diffusion equation (1.1), corresponding to a singular perturbation of the Laplacian at the center of the reactive target. In contrast, we now develop matched asymptotic expansions of $p_{\text{ST}}(\boldsymbol{r},t)$ in Laplace transform space, working directly with the appropriate reaction model. To avoid the evaluation of a number of integrals we previously calculated in [1], we do not calculate the expansions through term by term matching. Instead, we define one inner solution and one outer solution that encompass all terms needed to calculate the expansion of $p_{\text{ST}}(\boldsymbol{r},t)$ through $O(\varepsilon^2)$. We then match these two solutions, and show that the outer solution satisfies the same integral equation we found in [1], but with $\hat{k}_{\text{S}}$ replaced by the appropriate $\hat{k}$ for each reactive model. The analysis of [1] then gives the corresponding regular perturbation expansions of this integral equation, which in turn provides the expansion of $p_{\text{ST}}(\boldsymbol{r},t)$ through $O(\varepsilon^2)$. Note, while we take this approach to avoid repeating much of the analysis of [1], we expect one could alternatively match inner and outer solutions in Laplace transform space term by term and obtain the same final expansion (through $O(\varepsilon^2)$).

We begin by applying the Laplace transform to the governing equation (1.1), giving

$$\begin{aligned}(D\Delta - s)\,\tilde{p}_{\text{ST}}(\boldsymbol{r},s) &= -p_{\text{ST}}(\boldsymbol{r},0), \quad \boldsymbol{r}\in\Omega_{\text{free}},\, s>0,\\ \partial_{\boldsymbol{\eta}}\tilde{p}_{\text{ST}}(\boldsymbol{r},s) &= 0, \quad \boldsymbol{r}\in\partial\Omega,\, s>0,\end{aligned} \tag{2.30}$$

where the projected initial condition, $p_{\text{ST}}(\boldsymbol{r},0)$, is given by (2.4). Note that $p_{\text{ST}}(\boldsymbol{r},0)$ will depend on ε through the principal eigenfunction contribution, $\psi(\boldsymbol{r})\psi(\boldsymbol{r}_0)$. Equation (2.30) is coupled to the corresponding Laplace-transformed versions of the reactive models (1.2),(1.5), or (1.8).

To construct an inner solution we change variables as in the previous section, taking $\boldsymbol{y} = \frac{|\boldsymbol{r}-\boldsymbol{r}_{\text{b}}|}{\varepsilon}$. Denote by $\sigma(\boldsymbol{y},s)$ the corresponding inner expansion of $\tilde{p}_{\text{ST}}(\boldsymbol{r},s)$ near the reactive target. To determine an expansion of $p_{\text{ST}}(\boldsymbol{r},t)$ through $O(\varepsilon^2)$, we will require the first two terms in the expansion of $\sigma(\boldsymbol{y},s)$ (similar to how we only required $\phi^{(0)}$ and $\phi^{(1)}$ in the previous section). Let

$$\sigma(\boldsymbol{y},s) \sim w(\boldsymbol{y},s) := w^{(0)}(\boldsymbol{y},s) + \varepsilon w^{(1)}(\boldsymbol{y},s).$$

Assume $s = O(1)$. Substituting into (2.30) and changing to the $\boldsymbol{y}$ coordinate, we find $w(\boldsymbol{y},s)$ satisfies

$$\Delta w = 0, \quad |\boldsymbol{y}|>1, \tag{2.31}$$

with the pure absorption Dirichlet boundary condition

$$w(\boldsymbol{y},s) = 0, \quad |\boldsymbol{y}| = 1,$$

the partial absorption Robin boundary condition

$$-\partial_{\boldsymbol{\eta}} w(\boldsymbol{y},s) = \hat{\gamma} w(\boldsymbol{y},s), \quad |\boldsymbol{y}| = 1,$$

or the Doi reaction mechanism

$$-\Delta w(\boldsymbol{y}, s) + \hat{\mu} w(\boldsymbol{y}, s) = 0, \quad |\boldsymbol{y}| < 1.$$

In what follows, we will assume (2.31) is the correct asymptotic order equation for $w(\boldsymbol{y}, s)$ for all $s > 0$. That is, we assume any additional terms arising when s is large, i.e. $s = O(\varepsilon^{-\beta})$ for $\beta > 0$, can be ignored. One might expect this assumption to ultimately lead to an incorrect final expansion of $p(\boldsymbol{r}, t)$ for short times. In Section 2.5 we demonstrate that for short times, i.e. $t = O(\varepsilon^{\beta})$ with $\beta > 0$, the error introduced by this approximation does not change the asymptotic order of our final expansion of $p(\boldsymbol{r}, t)$.

For each reaction model w satisfies the same equation as the inner eigenfunction expansions, $\phi^{(i)}(\boldsymbol{y})$, studied in the previous section. We therefore conclude that

$$w(\boldsymbol{y}, s) = w_{\infty}(s; \varepsilon) \left(1 - \frac{\hat{k}}{\hat{k}_{\mathrm{S}}} \frac{1}{|\boldsymbol{y}|}\right), \quad |\boldsymbol{y}| > 1, \tag{2.32}$$

where $\hat{k}_{\mathrm{S}} = 4\pi D$ and the constant w_{∞} is determined by matching to the outer solution and can be written

$$w_{\infty}(s; \varepsilon) = w_{\infty}^{(0)}(s) + \varepsilon w_{\infty}^{(1)}(s).$$

We abuse notation, and subsequently denote by $\tilde{p}_{\mathrm{ST}}(\boldsymbol{r}, s)$ the expansion of the outer problem solution through terms of second order, i.e.

$$\tilde{p}_{\mathrm{ST}}(\boldsymbol{r}, s) := \tilde{p}_{\mathrm{ST}}^{(0)}(\boldsymbol{r}, s) + \varepsilon \tilde{p}_{\mathrm{ST}}^{(1)}(\boldsymbol{r}, s) + \varepsilon^2 \tilde{p}_{\mathrm{ST}}^{(2)}(\boldsymbol{r}, s),$$

where

$$\tilde{p}_{\mathrm{ST}}^{(0)}(\boldsymbol{r}, s) = \mathcal{L}\left[G(\boldsymbol{r}, \boldsymbol{r}_0, t) - \frac{1}{|\Omega|}\right] = \tilde{G}(\boldsymbol{r}, \boldsymbol{r}_0, s) - \frac{1}{|\Omega|\, s}$$

corresponds to the $\varepsilon = 0$ solution. The outer solution expansion then satisfies

$$\begin{aligned} (D\Delta - s)\tilde{p}_{\mathrm{ST}}(\boldsymbol{r}, s) &= -p_0(\boldsymbol{r}), \quad \boldsymbol{r} \in \Omega \setminus \{\boldsymbol{r}_{\mathrm{b}}\}, \\ \partial_{\boldsymbol{\eta}} \tilde{p}_{\mathrm{ST}}(\boldsymbol{r}, s) &= 0, \quad \boldsymbol{r} \in \partial\Omega, \end{aligned}$$

where $p_0(\boldsymbol{r})$ denotes the truncated asymptotic expansion of $p_{\mathrm{ST}}(\boldsymbol{r}, 0)$ as $\varepsilon \to 0$ through terms of $O(\varepsilon^2)$. That is

$$\begin{aligned} p_{\mathrm{ST}}(\boldsymbol{r}, 0) \sim p_0(\boldsymbol{r}) &:= p_{\mathrm{ST}}^{(0)}(\boldsymbol{r}, 0) + \varepsilon p_{\mathrm{ST}}^{(1)}(\boldsymbol{r}, 0) + \varepsilon^2 p_{\mathrm{ST}}^{(2)}(\boldsymbol{r}, 0), \\ &= \delta(\boldsymbol{r} - \boldsymbol{r}_0) - \left[\frac{1}{|\Omega|} + p_{\mathrm{LT}}^{(1)}(\boldsymbol{r}, \boldsymbol{r}_0, 0)\, \varepsilon + p_{\mathrm{LT}}^{(2)}(\boldsymbol{r}, \boldsymbol{r}_0, 0)\, \varepsilon^2\right]. \end{aligned}$$

As in the previous section, the singular behavior of $w(\boldsymbol{y}, s)$ as $|\boldsymbol{y}| \to \infty$ determines the singular behavior of $\tilde{p}_{\mathrm{ST}}(\boldsymbol{r}, s)$ as $\boldsymbol{r} \to \boldsymbol{r}_{\mathrm{b}}$. We find

$$\tilde{p}_{\mathrm{ST}}(\boldsymbol{r}, s) \sim -\frac{\varepsilon \hat{k}\, w_{\infty}(s; \varepsilon)}{\hat{k}_{\mathrm{S}}\, |\boldsymbol{r} - \boldsymbol{r}_{\mathrm{b}}|}, \quad \boldsymbol{r} \to \boldsymbol{r}_{\mathrm{b}}, \tag{2.33}$$

or equivalently, $\tilde{p}_{\text{ST}}(\boldsymbol{r}, s)$ satisfies

$$(D\Delta - s)\tilde{p}_{\text{ST}}(\boldsymbol{r}, s) = -p_0(\boldsymbol{r}) - \tilde{f}(s)\delta(\boldsymbol{r} - \boldsymbol{r}_{\text{b}}), \tag{2.34}$$

for some unknown source term, $\tilde{f}(s)$, that enforces the desired singular behavior. The solution is

$$\tilde{p}_{\text{ST}}(\boldsymbol{r}, s) = \int_{\Omega} \tilde{G}(\boldsymbol{r}, \boldsymbol{r}', s) p_0(\boldsymbol{r}') d\boldsymbol{r}' + \tilde{f}(s)\tilde{G}(\boldsymbol{r}, \boldsymbol{r}_{\text{b}}, s). \tag{2.35}$$

We rewrite $\tilde{p}_{\text{ST}}$ by explicitly removing the singular behavior as $\boldsymbol{r} \to \boldsymbol{r}_{\text{b}}$,

$$\tilde{p}_{\text{ST}}(\boldsymbol{r}, s) = \tilde{\varphi}(\boldsymbol{r}, s) + \tilde{h}(s) U(\boldsymbol{r}, \boldsymbol{r}_{\text{b}}), \tag{2.36}$$

where $\tilde{h}(s)$ is also an unknown function. The formal justification of this representation was shown in Appendix A of [1] for the pure-absorption Dirichlet boundary condition reactive model.

We now derive a well-defined integral equation for $\varphi(\boldsymbol{r}, t)$, to which regular perturbation theory can be applied to calculate the asymptotic expansions of $\tilde{\varphi}$, $\tilde{h}$, and hence $\tilde{p}_{\text{ST}}$. As part of our analysis we verify that $\tilde{\varphi}(\boldsymbol{r}, s)$ is indeed bounded as $\boldsymbol{r} \to \boldsymbol{r}_{\text{b}}$ for each $s > 0$.

The unknown function $\tilde{h}$ is determined by the matching condition (2.33). We find

$$w_{\infty}(s; \varepsilon) = \frac{-\tilde{h}(s)}{\varepsilon \hat{k}}. \tag{2.37}$$

To match the inner and outer solutions, we require

$$\lim_{\boldsymbol{r} \to \boldsymbol{r}_{\text{b}}} \left[\tilde{p}_{\text{ST}}(\boldsymbol{r}, s) - \frac{\tilde{h}(s)}{\hat{k}_{\text{S}} \left| \boldsymbol{r} - \boldsymbol{r}_{\text{b}} \right|} \right] = \lim_{|\boldsymbol{y}| \to \infty} w(\boldsymbol{y}, s),$$

which can be rewritten as

$$\tilde{\varphi}(\boldsymbol{r}_{\text{b}}, s) + \tilde{h}(s) R_0(\boldsymbol{r}_{\text{b}}, \boldsymbol{r}_{\text{b}}) = w_{\infty}(s; \varepsilon). \tag{2.38}$$

Combining (2.37) and (2.38) we obtain

$$\tilde{h}(s) = \frac{-\varepsilon \hat{k} \tilde{\varphi}(\boldsymbol{r}_{\text{b}}, s)}{1 + \varepsilon \hat{k} R_0(\boldsymbol{r}_{\text{b}}, \boldsymbol{r}_{\text{b}})}. \tag{2.39}$$

Hence,

$$\tilde{p}_{\text{ST}}(\boldsymbol{r}, s) = \tilde{\varphi}(\boldsymbol{r}, s) - \frac{\varepsilon \hat{k} \tilde{\varphi}(\boldsymbol{r}_{\text{b}}, s)}{1 + \varepsilon \hat{k} R_0(\boldsymbol{r}_{\text{b}}, \boldsymbol{r}_{\text{b}})} U(\boldsymbol{r}, \boldsymbol{r}_{\text{b}}) \tag{2.40}$$

is an asymptotic approximation to the solution of (2.30). Substituting (2.36) into (2.35) yields

$$\tilde{\varphi}(\boldsymbol{r}, s) + \tilde{h}(s) U(\boldsymbol{r}, \boldsymbol{r}_{\text{b}}) = \int_{\Omega} \tilde{G}(\boldsymbol{r}, \boldsymbol{r}', s) p_0(\boldsymbol{r}') d\boldsymbol{r}' + \tilde{f}(s)\tilde{G}(\boldsymbol{r}, \boldsymbol{r}_{\text{b}}, s). \tag{2.41}$$

In Appendix A we show that

$$\lim_{\boldsymbol{r}\to\boldsymbol{r}_\mathrm{b}}\left|\int_\Omega \tilde{G}(\boldsymbol{r},\boldsymbol{r}',s)p_0(\boldsymbol{r}')d\boldsymbol{r}'\right|<\infty,\quad \forall s>0, \tag{2.42}$$

so that the unknown function $\tilde{f}$ can be determined by requiring the singular terms to cancel in the limit $\boldsymbol{r}\to\boldsymbol{r}_\mathrm{b}$. That is, as $\boldsymbol{r}\to\boldsymbol{r}_\mathrm{b}$ we require

$$\tilde{h}(s)U(\boldsymbol{r},\boldsymbol{r}_\mathrm{b})=\tilde{h}(s)\left(R_0(\boldsymbol{r},\boldsymbol{r}_\mathrm{b})+\frac{1}{\hat{k}_\mathrm{S}\,|\boldsymbol{r}-\boldsymbol{r}_\mathrm{b}|}\right)\sim\tilde{f}(s)\tilde{G}(\boldsymbol{r},\boldsymbol{r}_\mathrm{b},s)\sim\frac{\tilde{f}(s)}{\hat{k}_\mathrm{S}\,|\boldsymbol{r}-\boldsymbol{r}_\mathrm{b}|},$$

implying $\tilde{f}(s)=\tilde{h}(s)$. We then find that $\tilde{\varphi}$ satisfies

$$\tilde{\varphi}(\boldsymbol{r},s)=\int_\Omega\tilde{G}(\boldsymbol{r},\boldsymbol{r}',s)p_0(\boldsymbol{r}')d\boldsymbol{r}'-\frac{\varepsilon\hat{k}\tilde{\varphi}(\boldsymbol{r}_\mathrm{b},s)}{1+\varepsilon\hat{k}R_0(\boldsymbol{r}_\mathrm{b},\boldsymbol{r}_\mathrm{b})}\left[\tilde{G}(\boldsymbol{r},\boldsymbol{r}_\mathrm{b},s)-U(\boldsymbol{r},\boldsymbol{r}_\mathrm{b})\right]. \tag{2.43}$$

For each $s>0$ this corresponds to the Laplace transform of the time-domain integral equation we derived in [1] when $\hat{k}=\hat{k}_\mathrm{S}$,

$$\begin{aligned}\varphi(\boldsymbol{r},t)=&\int_\Omega G(\boldsymbol{r},\boldsymbol{r}',t)p_0(\boldsymbol{r}')d\boldsymbol{r}'\\&+\frac{\varepsilon\hat{k}}{1+\varepsilon\hat{k}R_0(\boldsymbol{r}_\mathrm{b},\boldsymbol{r}_\mathrm{b})}\left(U(\boldsymbol{r},\boldsymbol{r}_\mathrm{b})\varphi(\boldsymbol{r}_\mathrm{b},t)-\int_0^t G(\boldsymbol{r},\boldsymbol{r}_\mathrm{b},t-s)\varphi(\boldsymbol{r}_\mathrm{b},s)ds\right),\end{aligned} \tag{2.44}$$

see equation (2.33) in [1]. Recalling (2.40), we conclude that the perturbation expansion as $\varepsilon\to0$ of this integral equation developed in [1] determines the corresponding expansion of $p_{\mathrm{ST}}(\boldsymbol{r},t)$ by simply replacing $\hat{k}_\mathrm{S}$ with $\hat{k}$. For completeness we now summarize that expansion.

Principal Result 2.2. *The asymptotic expansion of $p_{ST}(\boldsymbol{r},t)$ as $\varepsilon\to0$ is given by*

$$\begin{aligned}p_{ST}^{(0)}(\boldsymbol{r},t)&=G(\boldsymbol{r},\boldsymbol{r}_0,t)-\frac{1}{|\Omega|},\\p_{ST}^{(1)}(\boldsymbol{r},t)&=-\hat{k}\int_0^t G(\boldsymbol{r},\boldsymbol{r}_\mathrm{b},t-s)p_{ST}^{(0)}(\boldsymbol{r}_\mathrm{b},s)\,ds+\frac{\hat{k}}{|\Omega|}U(\boldsymbol{r}_0,\boldsymbol{r}_\mathrm{b})\\&\qquad+\frac{\hat{k}}{|\Omega|}\int_\Omega G(\boldsymbol{r},\boldsymbol{r}',t)U(\boldsymbol{r}',\boldsymbol{r}_\mathrm{b})\,d\boldsymbol{r}',\end{aligned}$$

with $p_{ST}^{(2)}(\boldsymbol{r},t)$ given by (2.39c) of [1].

Remark 2.1. *In the limit $\boldsymbol{r}\to\boldsymbol{r}_\mathrm{b}$* (2.43) *becomes*

$$\tilde{\varphi}(\boldsymbol{r}_\mathrm{b},s)=\int_\Omega\tilde{G}(\boldsymbol{r}_\mathrm{b},\boldsymbol{r}',s)p_0(\boldsymbol{r}')d\boldsymbol{r}'-\frac{\varepsilon\hat{k}\tilde{\varphi}(\boldsymbol{r}_\mathrm{b},s)}{1+\varepsilon\hat{k}R_0(\boldsymbol{r}_\mathrm{b},\boldsymbol{r}_\mathrm{b})}\left(\tilde{R}(\boldsymbol{r}_\mathrm{b},\boldsymbol{r}_\mathrm{b},s)-R_0(\boldsymbol{r}_\mathrm{b},\boldsymbol{r}_\mathrm{b})-\sqrt{\frac{s}{D\hat{k}^2}}\right).$$

Solving for $\tilde{\varphi}(\boldsymbol{r}_b, s)$ yields

$$\tilde{\varphi}(\boldsymbol{r}_b, s) = \frac{1 + \varepsilon\hat{k}R_0(\boldsymbol{r}_b, \boldsymbol{r}_b)}{1 + \varepsilon\hat{k}\tilde{R}(\boldsymbol{r}_b, \boldsymbol{r}_b, s) - \varepsilon\sqrt{\frac{s}{D}}} \int_\Omega \tilde{G}(\boldsymbol{r}_b, \boldsymbol{r}', s) p_0(\boldsymbol{r}') d\boldsymbol{r}'. \tag{2.46}$$

Substituting (2.46) *into* (2.43) *we obtain an explicit formula for $\tilde{\varphi}(\boldsymbol{r}, s)$, and hence $\tilde{p}_{ST}(\boldsymbol{r}, s)$. However, inverting* (2.46) *seems less practical then developing regular perturbation expansions of* (2.44) *as in [1].*

2.4 Summary of complete expansions

Combining (2.29) with Result 2.2, we obtain a complete expansion of $p(\boldsymbol{r}, t)$ through terms of $O(\varepsilon^2)$ for each reactive model. The expansion is identical to that obtained in [1] for the pure absorption Smoluchowski reaction where $\hat{k} = \hat{k}_S$. To obtain expansions for either the partial absorption or Doi reaction mechanisms, one need only substitute the appropriate diffusion limited rate $\hat{k}_R$ or $\hat{k}_D$, given by (2.6) and (2.7). In the remainder we only utilize the expansion through terms of $O(\varepsilon)$. We therefore omit higher order terms here, and direct the interested reader to [1] for the complete expansion formulas through $O(\varepsilon^2)$.

Principal Result 2.3. *The asymptotic expansion of $p(\boldsymbol{r}, t)$ as $\varepsilon \to 0$ through terms of $O(\varepsilon)$ is*

$$\begin{aligned} p(\boldsymbol{r}, t) \sim G(\boldsymbol{r}, \boldsymbol{r}_0, t) - \frac{1}{|\Omega|}\left(1 - e^{-\lambda_{LT} D t}\right) - \varepsilon\hat{k}\int_0^t G(\boldsymbol{r}, \boldsymbol{r}_b, t-s)\left(G(\boldsymbol{r}_b, \boldsymbol{r}_0, s) - \frac{1}{|\Omega|}\right) ds \\ + \frac{\varepsilon\hat{k}}{|\Omega|}\left[\int_\Omega G(\boldsymbol{r}, \boldsymbol{r}', t) U(\boldsymbol{r}', \boldsymbol{r}_b) d\boldsymbol{r}' - U(\boldsymbol{r}, \boldsymbol{r}_b) e^{-\lambda_{LT} D t} + (1 - e^{-\lambda_{LT} D t}) U(\boldsymbol{r}_0, \boldsymbol{r}_b)\right]. \end{aligned} \tag{2.47}$$

In many biological problems, statistics of the first passage time for a reaction to occur are of particular interest. Denote by $f(t)$ the corresponding probability density function for the first passage time. It is related to $p(\boldsymbol{r}, t)$ by

$$f(t) = -\frac{d}{dt}\int_\Omega p(\boldsymbol{r}, t) d\boldsymbol{r}. \tag{2.48}$$

Using Result 2.3, the expansion of $f(t)$ can be derived as in [1]. We find

Principal Result 2.4. *The asymptotic expansion of $f(t)$ as $\varepsilon \to 0$ through terms of $O(\varepsilon)$ is*

$$f(t) \sim \left(1 - \varepsilon\hat{k}U(\boldsymbol{r}_0, \boldsymbol{r}_b)\right)\lambda_{LT} D e^{-\lambda_{LT} D t} + \varepsilon\hat{k}\left(G(\boldsymbol{r}_b, \boldsymbol{r}_0, t) - \frac{1}{|\Omega|}\right), \tag{2.49}$$

where λ_{LT} is the asymptotic expansion of the principal eigenvalue given by (2.26).

With substitution of the appropriate $\hat{k}$ for $\hat{k}_S$, the complete expansion through terms of $O(\varepsilon^2)$ is given by (2.49) of [1].

Remark 2.2. *Suppose $\hat{\gamma}$ or $\hat{\mu}$ is chosen so that the diffusion limited rates in the partial absorption and Doi models are the same, $\hat{k}_R = \hat{k}_D$. The final expansion formulas for $p(\boldsymbol{r}, t)$ and $f(t)$ are then identical. For irreversible bimolecular reactions, this demonstrates that when ε is a small parameter the two models are practically equivalent.*

2.5 Short time correctness of (2.47)

In deriving the asymptotic expansion of the short time correction given in (2.2) we made the approximation that the large s contribution in (2.31) could be ignored (i.e. when $s = O(\varepsilon^{-\beta})$ for $\beta > 0$). This might lead to the suspicion that the expansion of $p(\boldsymbol{r}, t)$ given by (2.47) may be incorrect for sufficiently small times (i.e. $t = O(\varepsilon^{\beta})$ for $\beta > 0$). In this section we demonstrate that on such short timescales, the error between $p(\boldsymbol{r}, t)$ and the expansion (2.47) is at most $O(\varepsilon^{2+\beta})$.

For simplicity, we will restrict attention to the error introduced in the asymptotic expansion of the solution to the Doi problem, $p(\boldsymbol{r}, t)$ satisfying (1.1) with the reactive term (1.6) and the initial condition, $p(\boldsymbol{r}, 0) = \delta(\boldsymbol{r} - \boldsymbol{r}_0)$. To make explicit the ε dependence of $p(\boldsymbol{r}, t)$, we will subsequently write $p_\varepsilon(\boldsymbol{r}, t)$. With this notation, $p_0(\boldsymbol{r}, t) = G(\boldsymbol{r}, \boldsymbol{r}_0, t)$ will then denote the solution to the corresponding $\varepsilon = 0$ pure-diffusion problem in which there is no reactive target. Finally, in what follows we denote by $\rho_\varepsilon(\boldsymbol{r}, t)$ the corresponding truncated first order expansion given by the right hand side of (2.47).

To examine the short-time behavior of $\rho_\varepsilon(\boldsymbol{r}, t)$, we will find it convenient to rewrite (2.47). Using (2.11), Fubini's Theorem and the semigroup property of $G(\boldsymbol{r}, \boldsymbol{r}', t)$ we have the identity that

$$\begin{aligned}
\int_\Omega G(\boldsymbol{r}, \boldsymbol{r}', t) U(\boldsymbol{r}', \boldsymbol{r}_b)\, d\boldsymbol{r}' &= \int_0^\infty \int_\Omega G(\boldsymbol{r}, \boldsymbol{r}', t) \left[G(\boldsymbol{r}', \boldsymbol{r}_b, s) - \frac{1}{|\Omega|} \right] d\boldsymbol{r}'\, ds, \\
&= \int_t^\infty \left[G(\boldsymbol{r}, \boldsymbol{r}_b, s) - \frac{1}{|\Omega|} \right] ds, \\
&= U(\boldsymbol{r}, \boldsymbol{r}_b) - \int_0^t \left[G(\boldsymbol{r}, \boldsymbol{r}_b, s) - \frac{1}{|\Omega|} \right] ds, \\
&= U(\boldsymbol{r}, \boldsymbol{r}_b) - \int_0^t G(\boldsymbol{r}, \boldsymbol{r}_b, s)\, ds + \frac{t}{|\Omega|}.
\end{aligned}$$

Using this identity we can simplify (2.47) to

$$\begin{aligned}
\rho_\varepsilon(\boldsymbol{r}, t) = G(\boldsymbol{r}, \boldsymbol{r}_0, t) + \frac{1}{|\Omega|} \left(1 - e^{-\lambda_{\mathrm{LT}} D t} \right) \left[-1 + \varepsilon \hat{k} \left(U(\boldsymbol{r}, \boldsymbol{r}_b) + U(\boldsymbol{r}_0, \boldsymbol{r}_b) \right) \right] \\
+ \frac{\varepsilon \hat{k} t}{|\Omega|^2} - \varepsilon \hat{k} \int_0^t G(\boldsymbol{r}, \boldsymbol{r}_b, t - s) G(\boldsymbol{r}_b, \boldsymbol{r}_0, s) ds. \quad (2.50)
\end{aligned}$$

Let

$$d(\boldsymbol{r}, \Omega_\varepsilon) = \inf_{\boldsymbol{r}' \in \Omega_\varepsilon} \left| \boldsymbol{r} - \boldsymbol{r}' \right|$$

denote the distance of $\boldsymbol{r}$ from the target, Ω_ε. Our goal is to demonstrate the following:

Theorem 2.1. *For all $\varepsilon > 0$ sufficiently small, when $t = O(\varepsilon^{\beta})$ with $\beta > 0$, then*

$$p_\varepsilon(\boldsymbol{r}, t) = \rho_\varepsilon(\boldsymbol{r}, t) + O(\varepsilon^{2+\beta}), \quad (2.51)$$

for all $\boldsymbol{r}$ and $\boldsymbol{r}_0$ in Ω such that

$$\min\{d(\boldsymbol{r},\Omega_\varepsilon), d(\boldsymbol{r}_0,\Omega_\varepsilon)\} > C > 0, \tag{2.52}$$

for any positive constant C independent of ε. That is, provided we start the particle $O(1)$ from the target and examine the solution $O(1)$ from the target, for short times we expect the error between the asymptotic expansion and the true solution to the Doi problem to be higher then second order in ε.

In establishing this result we will make use of the following lemma, which is proven in Appendix B.

Lemma 2.1. *$p_\varepsilon(\boldsymbol{r},t)$ and $G(\boldsymbol{r},\boldsymbol{r}',t)$ have the following basic properties:*

1. *The Doi solutions monotonically increase as ε decreases. That is, assuming $p_{\varepsilon_1}(\boldsymbol{r},0) = p_{\varepsilon_2}(\boldsymbol{r},0) = p_0(\boldsymbol{r},0)$,*
$$p_{\varepsilon_2}(\boldsymbol{r},t) \le p_{\varepsilon_1}(\boldsymbol{r},t) \le p_0(\boldsymbol{r},t), \quad 0 \le \varepsilon_1 \le \varepsilon_2. \tag{2.53}$$
2. *Assume the domain Ω is sufficiently regular (at least Lipschitz, see [17]). For t in $[0,1]$ there are constants, $c_1 > 0$ and $c_2 > 0$, such that the $\varepsilon = 0$ diffusion equation Green's function, $G(\boldsymbol{r},\boldsymbol{r}',t)$, satisfies the bound*
$$G(\boldsymbol{r},\boldsymbol{r}',t) \le \frac{c_1}{t^{3/2}} e^{-|\boldsymbol{r}-\boldsymbol{r}'|^2/c_2 t}. \tag{2.54}$$

With the preceding lemma we are ready to establish our main result

Proof of Theorem 2.1. As

$$|p_\varepsilon(\boldsymbol{r},t) - \rho_\varepsilon(\boldsymbol{r},t)| \le |G(\boldsymbol{r},\boldsymbol{r}_0,t) - \rho_\varepsilon(\boldsymbol{r},t)| + |G(\boldsymbol{r},\boldsymbol{r}_0,t) - p_\varepsilon(\boldsymbol{r},t)|,$$

it is sufficient to show that both

$$G(\boldsymbol{r},\boldsymbol{r}_0,t) - \rho_\varepsilon(\boldsymbol{r},t) = O(\varepsilon^{2+\beta}), \tag{2.55}$$

and

$$G(\boldsymbol{r},\boldsymbol{r}_0,t) - p_\varepsilon(\boldsymbol{r},t) = O(\varepsilon^{2+\beta}). \tag{2.56}$$

We begin with (2.55). Recalling the definition of λ_{LT}, (2.26), for $t = O(\varepsilon^\beta)$ we have that

$$1 - e^{-\lambda_{\text{LT}} D t} = \frac{\hat{k}\varepsilon t}{|\Omega|} + O(\varepsilon^{2+\beta}),$$

so that

$$G(\boldsymbol{r},\boldsymbol{r}_0,t) - \rho_\varepsilon(\boldsymbol{r},t) = -\varepsilon\hat{k}\left[\frac{\varepsilon\hat{k}t}{|\Omega|^2} + O(\varepsilon^{2+\beta})\right][U(\boldsymbol{r},\boldsymbol{r}_b) + U(\boldsymbol{r}_0,\boldsymbol{r}_b)] + O(\varepsilon^{2+\beta}) + \varepsilon\hat{k}\int_0^t G(\boldsymbol{r},\boldsymbol{r}_b,t-s)G(\boldsymbol{r}_b,\boldsymbol{r}_0,s)ds.$$

The assumption that $d(\boldsymbol{r}, \Omega_\varepsilon) > C$ and $d(\boldsymbol{r}_0, \Omega_\varepsilon) > C$, for some $C > 0$ independent of ε, implies that $|\boldsymbol{r} - \boldsymbol{r}_\mathrm{b}| > C$ and $|\boldsymbol{r}_0 - \boldsymbol{r}_\mathrm{b}| > C$. By (2.10), this assumption implies that $U(\boldsymbol{r}, \boldsymbol{r}_\mathrm{b})$ and $U(\boldsymbol{r}_0, \boldsymbol{r}_\mathrm{b})$ are both uniformly bounded by constants independent of ε. As such, the right hand side of the first line is $O(\varepsilon^{2+\beta})$. We claim that the integral on the second line is exponentially small in ε, which immediately implies (2.55).

By (2.54)

$$\begin{aligned}\int_0^t G(\boldsymbol{r}, \boldsymbol{r}_\mathrm{b}, t-s) G(\boldsymbol{r}_\mathrm{b}, \boldsymbol{r}_0, s)\, ds &\leq c_1^2 \int_0^t \frac{1}{(t-s)^{3/2} s^{3/2}} e^{-|\boldsymbol{r}-\boldsymbol{r}_\mathrm{b}|^2/c_2(t-s)} e^{-|\boldsymbol{r}_\mathrm{b}-\boldsymbol{r}_0|^2/c_2 s}\, ds \\ &= \frac{c_1^2 \sqrt{c_2 \pi}\, (|\boldsymbol{r}-\boldsymbol{r}_\mathrm{b}| + |\boldsymbol{r}_\mathrm{b}-\boldsymbol{r}_0|)}{|\boldsymbol{r}-\boldsymbol{r}_\mathrm{b}|\, |\boldsymbol{r}_\mathrm{b}-\boldsymbol{r}_0|} \frac{1}{t^{3/2}} e^{-(|\boldsymbol{r}-\boldsymbol{r}_\mathrm{b}|+|\boldsymbol{r}_\mathrm{b}-\boldsymbol{r}_0|)^2/c_2 t}.\end{aligned}$$

Here the last line follows by Laplace transforming the time convolution, combining terms, and then inverse transforming. Using (2.52) and the boundedness of Ω, we find

$$\int_0^t G(\boldsymbol{r}, \boldsymbol{r}_\mathrm{b}, t-s) G(\boldsymbol{r}_\mathrm{b}, \boldsymbol{r}_0, s)\, ds \leq \frac{M}{t^{3/2}} e^{-2C^2/c_2 t},$$

for a positive constant, M, independent of t and ε. The inequality demonstrates that for all ε sufficiently small, the integral is exponentially small in ε when $t = O(\varepsilon^\beta)$, establishing (2.55).

Finally we establish (2.56). Let

$$v(\boldsymbol{r}, t) = G(\boldsymbol{r}, \boldsymbol{r}_0, t) - p_\varepsilon(\boldsymbol{r}, t),$$

which satisfies the diffusion equation

$$\begin{aligned}\frac{\partial v}{\partial t} &= D\Delta V + \mu \mathbb{1}_{\Omega_\varepsilon}(\boldsymbol{r}) p_\varepsilon(\boldsymbol{r}, t), \quad \boldsymbol{r} \in \Omega, t > 0 \\ \partial_{\boldsymbol{\eta}} v(\boldsymbol{r}, t) &= 0, \quad \boldsymbol{r} \in \partial\Omega, t > 0, \\ v(\boldsymbol{r}, 0) &= 0, \quad \boldsymbol{r} \in \Omega,\end{aligned}$$

where $\mathbb{1}_{\Omega_\varepsilon}(\boldsymbol{r})$ denotes the indicator function of the set Ω_ε. Using Duhamel's Principle we have

$$v(\boldsymbol{r}, t) = \mu \int_0^t \int_{\Omega_\varepsilon} G(\boldsymbol{r}, \boldsymbol{r}', t-s) p_\varepsilon(\boldsymbol{r}', s)\, d\boldsymbol{r}'\, ds.$$

Clearly $v(\boldsymbol{r}, t) \geq 0$. Recalling that $p_0(\boldsymbol{r}, t) = G(\boldsymbol{r}, \boldsymbol{r}_0, t)$, the monotonicity condition (2.53) then implies

$$|v(\boldsymbol{r}, t)| \leq \mu \int_0^t \int_{\Omega_\varepsilon} G(\boldsymbol{r}, \boldsymbol{r}', t-s) G(\boldsymbol{r}', \boldsymbol{r}_0, s)\, d\boldsymbol{r}'\, ds.$$

We now apply the bound (2.54) to each Green's function within the integrand, and use that $d(\boldsymbol{r}, \Omega_\varepsilon) > C$ and $d(\boldsymbol{r}_0, \Omega_\varepsilon) > C$, for some $C > 0$ independent of ε. Assuming that ε, and hence t, are sufficiently small we find

$$G(\boldsymbol{r}, \boldsymbol{r}', t-s) \leq \frac{c_1}{(t-s)^{3/2}} e^{-C^2/c_2(t-s)} \leq \frac{c_1}{t^{3/2}} e^{-C^2/c_2 t}, \qquad \text{for all } s \in [0,t]\,,$$
$$G(\boldsymbol{r}', \boldsymbol{r}_0, s) \leq \frac{c_1}{s^{3/2}} e^{-C^2/c_2 s} \leq \frac{c_1}{t^{3/2}} e^{-C^2/c_2 t}, \qquad \text{for all } s \in [0,t]\,.$$

Here we have used that for t sufficiently small, the Gaussian bounds are maximized in time at $s = 0$ and $s = t$ respectively. Using these bounds we see that

$$|v(\boldsymbol{r}, t)| \leq \mu \, |\Omega_\varepsilon| \, t \left(\frac{c_1}{t^{3/2}} e^{-C^2/c_2 t} \right)^2,$$

which is exponentially small in ε for $t = O(\varepsilon^\beta)$. We therefore find that (2.56) holds. □

Remark 2.3. *One could modify the proof to allow for general bounded initial conditions. While we do not show it here, we expect these modifications would not require the initial condition to be zero near Ω_ε, as was necessary for the delta source initial conditions we studied above. Instead, we expect that only the condition $d(\boldsymbol{r}, \Omega_\varepsilon) > C > 0$ should carry over.*

3 Results: spherical domain

3.1 Comparison of accuracy in the spherically symmetric problem

We illustrate the approximation for a spherical domain, with standard spherical coordinates (r, θ, φ), and the assumption that $D = 1$. Choosing Ω to be the unit sphere, we have that

$$G(\boldsymbol{r}, \boldsymbol{r}', t) = \frac{1}{|\Omega|} + \frac{1}{\pi^2} \sum_{n=1}^{\infty} \sum_{m=1}^{\infty} \frac{(2n+1)\alpha_m^3}{1/4 + \alpha_m^2 - (n+1/2)^2} P_n(\cos\theta) j_n(\alpha_m r) j_n(\alpha_m r') e^{-\alpha_m^2 t}, \tag{3.1}$$

where $P_n(.)$ are the Legendre polynomials and $j_n(.)$ are spherical Bessel functions [18, 19]. The Neumann Green's function is [19]

$$U(\boldsymbol{r}, \boldsymbol{r}') = \frac{1}{4\pi} \left[\frac{1}{\sqrt{r^2 - 2rr'\cos\theta + r'^2}} + \frac{1}{\sqrt{1 - 2rr'\cos\theta + r^2 r'^2}} \right] + \frac{1}{4\pi} \log\left(\frac{2}{1 - rr'\cos\theta + \sqrt{1 - 2rr'\cos\theta + r^2 r'^2}} \right) + \frac{r^2 + r'^2}{6\,|\Omega|} - \frac{7}{10\pi}. \tag{3.2}$$

We first explore the simplest case where the solution is radially symmetric. Here we can check the accuracy of our asymptotic expansions by direct comparison to exact solutions of the Robin

and Doi problems. We use the explicit solution formulas from [18, 19] and [15] respectively. The target is placed at the center of the sphere, and the diffusing molecule's initial position is uniformly distributed over the sphere of radius r_0. In this special case $G(\boldsymbol{r}, \boldsymbol{r}', t)$ can be simplified, see Ref. [1].

To compare each of the reaction mechanisms, we choose $\hat{\gamma}$ (the Robin constant) and $\hat{\mu}$ (the Doi absorption rate) so that the diffusion limited rates $\hat{k}_{\mathrm{R}}$ (2.6) and $\hat{k}_{\mathrm{D}}$ (2.7) are equal. With this choice the asymptotic expansions of the solutions for each reaction model are identical in the outer region (see the previous section).

In Fig. 1 we examine the difference between three first passage time densities: the exact Doi solution, $f_{\mathrm{doi}}(t)$, the exact Robin solution, $f_{\mathrm{rob}}(t)$, and the two term asymptotic approximation, $f_{\mathrm{asy}}(t)$ (i.e. truncated after terms of $O(\varepsilon)$). The max norm error between the two exact solutions and the approximation illustrates the accuracy of the asymptotic result, which converges like $O(\varepsilon)$ as expected. Since $\hat{\gamma}$ and $\hat{\mu}$ are chosen so that the two reaction mechanisms are comparable, we also show the max norm difference between the two exact solutions. When $\hat{\mu} = 1$ the effective reaction rate is low and the pairwise differences between the three solutions are similar in magnitude. When $\hat{\mu} = 100$ the reaction rate is increased and the exact solutions are closer to each other than they are to the approximation. Moreover, the difference between the exact solutions appears to approach zero faster as $\varepsilon \to 0$ than the difference between each exact solution and corresponding asymptotic expansion.

3.2 Comparison of accuracy in the non spherically symmetric problem

In Fig. 2 we break the radial symmetry by setting the target position to $\boldsymbol{r}_{\mathrm{b}} = (\theta_b, \phi_b, r_b) = (0, 0, 0.5)$ and examine the effect of changing the location of the initial position $\boldsymbol{r}_0$ on the first passage time density. Notice that in this example, the molecule starts at a specific point $\boldsymbol{r}_0$, whereas in the previous section, the molecule started at a uniformly distributed point over the sphere of radius r_0. Without radial symmetry, we no longer have exact solutions to validate the accuracy of the approximation so we use Monte Carlo simulations. The implementation of the Monte Carlo simulations is described in Appendix C. We see that the asymptotic approximations, which only include terms through $O(\varepsilon)$, become somewhat less accurate when the initial position approaches within a distance 0.5 of the target.

In Fig. 3 we look at more choices of initial position and target location with $|\boldsymbol{r}_{\mathrm{b}} - \boldsymbol{r}_0| = 0.7$ fixed. As expected, there is little to no loss of accuracy when $\boldsymbol{r}_0$ approaches the boundary. In contrast, we see that the approximation loses some accuracy when $\boldsymbol{r}_{\mathrm{b}}$ approaches the boundary. To improve accuracy in this case, when the target is $O(\varepsilon)$ from the boundary one could consider a more refined inner problem in which the target lives in a half-space above a plane (corresponding to the flattened boundary). If the target merges with the boundary, becoming a small hole, one would need to solve the related narrow escape problem [20, 9].

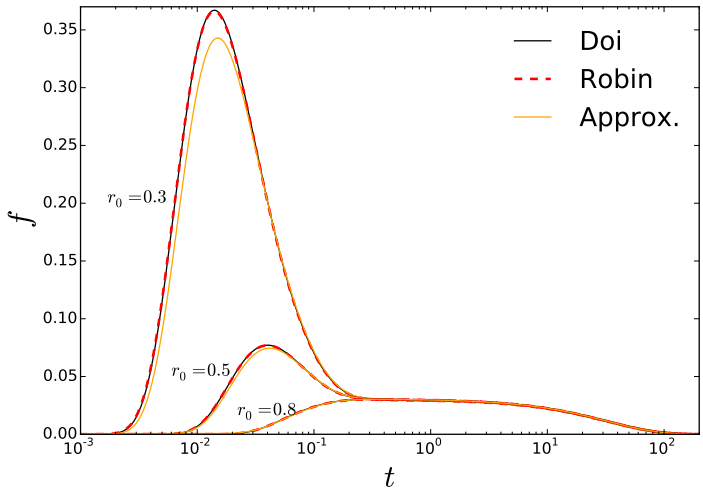

(a) The first passage time density ($\varepsilon = 0.01$).

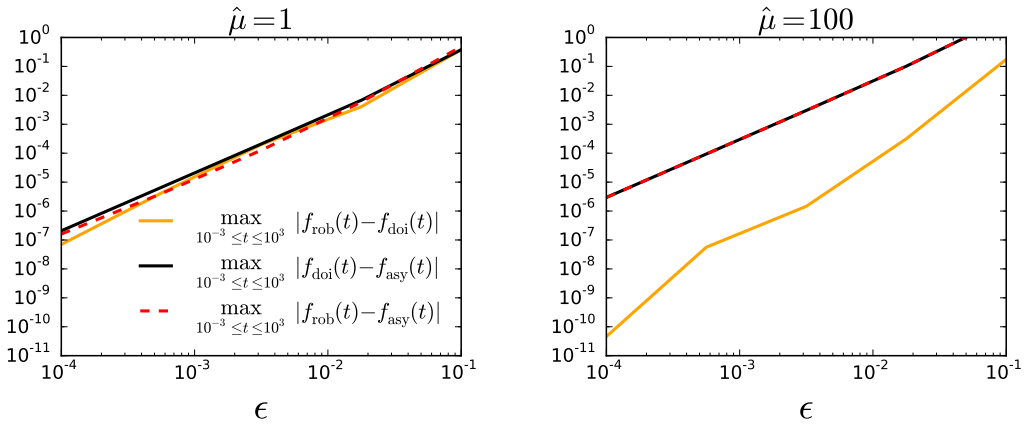
$\hat{\mu} = 1$
$\hat{\mu} = 100$
$\max_{10^{-3} \le t \le 10^3} |f_{\mathrm{rob}}(t) - f_{\mathrm{doi}}(t)|$
$\max_{10^{-3} \le t \le 10^3} |f_{\mathrm{doi}}(t) - f_{\mathrm{asy}}(t)|$
$\max_{10^{-3} \le t \le 10^3} |f_{\mathrm{rob}}(t) - f_{\mathrm{asy}}(t)|$
ϵ
ϵ

(b) The max norm difference between the first passage time densities ($r_0 = 0.3$).

Figure 1: Spherically symmetric first passage time density. We set $D = 1$ and $\hat{\gamma} = \sqrt{\hat{\mu}}/\tanh(\sqrt{\hat{\mu}}) - 1$. With these choices, $\hat{k}_{\mathrm{R}} = \hat{k}_{\mathrm{D}}$, so that solutions to the Robin and Doi models have identical asymptotic expansions through $O(\varepsilon^2)$.

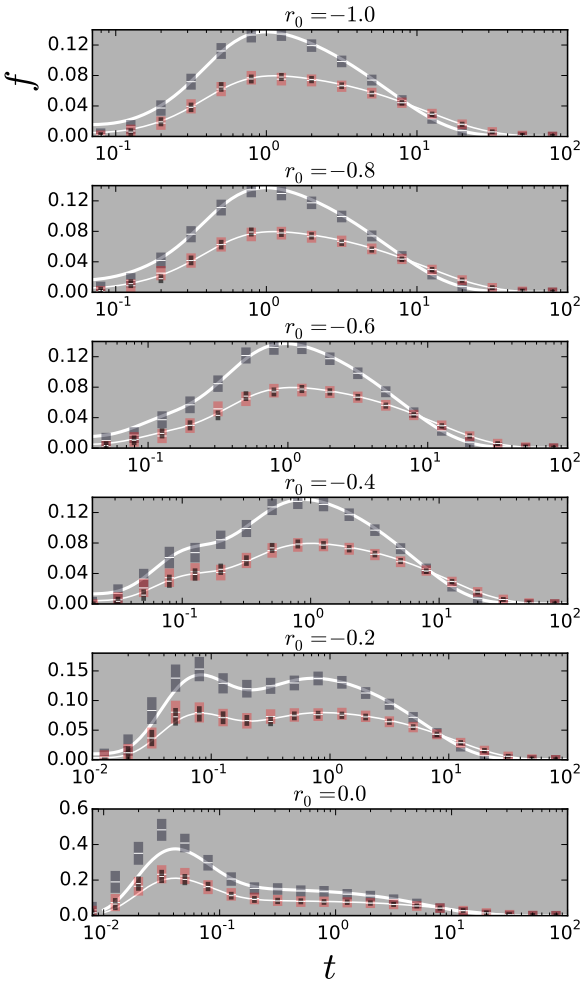

Figure 2: The first passage time density, with the target center fixed at $\boldsymbol{r}_b = (\theta_b, \phi_b, r_b) = (0, 0, 0.5)$. The initial position is $\boldsymbol{r}_0 = (0, 0, r_0)$. The approximations (solid lines) are compared to normalized histograms obtained from Monte Carlo simulations, which are plotted as rectangles centered at the histogram value. The height of each rectangle represents a 95% confidence interval. Thick white lines (gray rectangles) show the approximation of the pure absorption problem. Thin white lines correspond to the approximation of the Robin (red rectangles) and Doi (black rectangles) partial reaction mechanisms. Parameter values are $\varepsilon = 0.05$, $D = 1$, $\hat{\mu} = 5$, and $\hat{\gamma} = \sqrt{\hat{\mu}}/\tanh(\sqrt{\hat{\mu}}) - 1$.

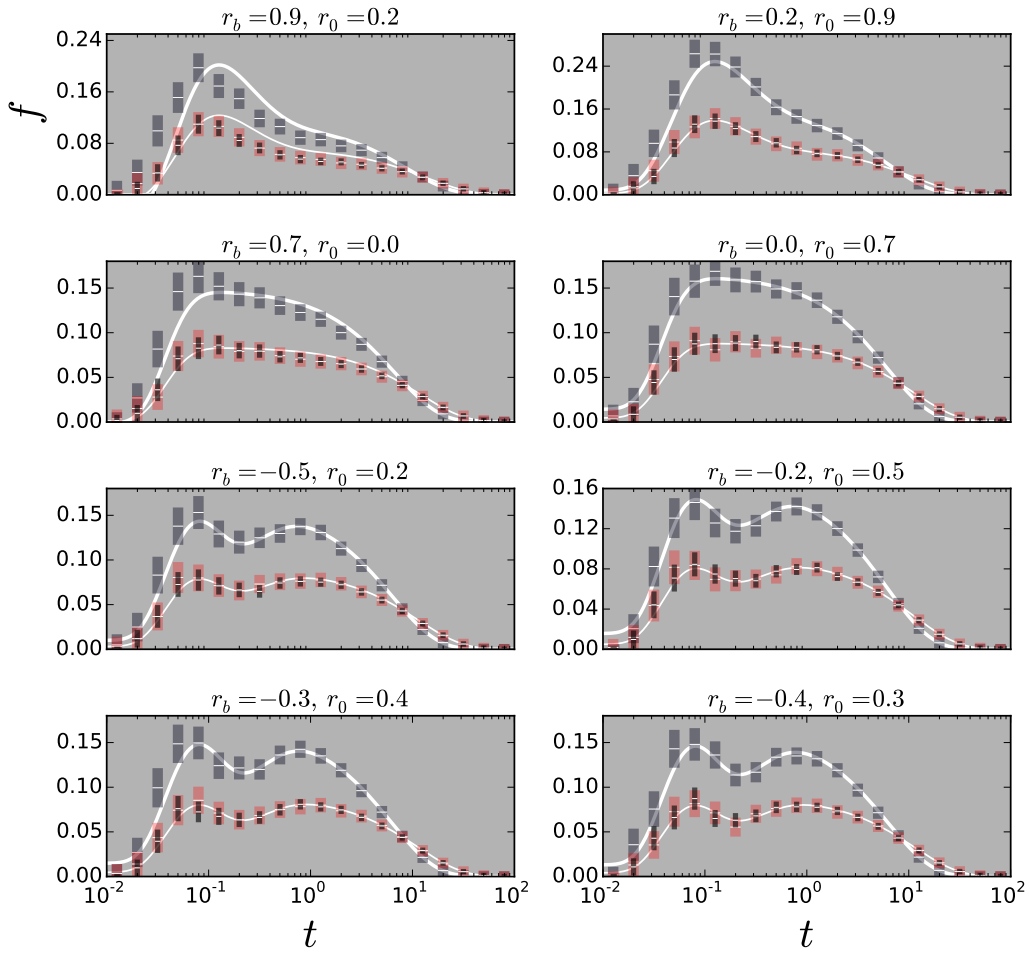

Figure 3: Same as Fig. 2 with different choices of the target location $\boldsymbol{r}_\mathrm{b}$ and initial position $\boldsymbol{r}_0$ such that $|\boldsymbol{r}_\mathrm{b} - \boldsymbol{r}_0| = 0.7$

3.3 Multiple timescales

Our analysis reveals three important timescales for the first passage time problem. The mean first passage time, $\tau_m \sim 1/\lambda$ (see Sec. 2.2), is the longest timescale and is independent of the initial condition; it is characterized by trajectories that explore a large fraction of the domain before reaching the target. Two other timescales, corresponding to the peaks seen in Fig. 2, are revealed by the short time contribution of our asymptotic approximation. We call these τ_g and τ_s, where $\tau_g \leq \tau_s \leq \tau_m$.

When $|\boldsymbol{r}_\mathrm{b} - \boldsymbol{r}_0| < 0.7$, the first-passage time density has a single peak at $\tau_g < 0.1$. For larger initial separations, $|\boldsymbol{r}_\mathrm{b} - \boldsymbol{r}_0| > 0.7$, there is again a single peak, but it occurs later, on the timescale of τ_s, with its maximum closer to $t = 1$. When $|\boldsymbol{r}_\mathrm{b} - \boldsymbol{r}_0| \approx 0.7$, both peaks are present and distinguishable from each other.

In Fig. 3, we examine different target positions with $|\boldsymbol{r}_\mathrm{b} - \boldsymbol{r}_0| = 0.7$ fixed. When the center of the sphere is between the starting position and the target, we see two peaks in the first passage time density. In contrast, when the target and the starting position are within the same hemisphere, there is a single broad peak encompassing both timescales. Note that in the top left pane that the target is within 2ε of the boundary, where our expansion is no longer valid. When the target is on the boundary, this situation is known as a narrow escape problem [21, 9, 22].

To understand what gives rise to the τ_g and τ_s timescales, we examine the approximation to the joint distribution $p(\boldsymbol{r}, t)$, which tells us what parts of the domain the molecule is likely to explore during the search. In Fig. 4 we set $\boldsymbol{r}_0 = (\theta_0, \phi_0, r_0) = (\pi, 0, 0.35)$ and $\boldsymbol{r}_\mathrm{b} = (0, 0, 0.35)$. For reference, the resulting first passage time density is shown in Fig. 4(a), which has two peaks corresponding to τ_g and τ_s. In Fig. 4(b), we show $p(\boldsymbol{r}, t)$ on the bottom half of the spherical domain at several different times. The top three snapshots show how probability arrives at the target as $t \to \tau_g$, and the bottom three snapshots show how probability arrives at the target as $t \to \tau_s$.

At $t = 0.05$ we see the initial Gaussian spread that is relatively unaffected by the boundary. Indicating that τ_g is characterized by trajectories that reach the target before encountering the boundary.

The bottom three snapshots, starting at $t = 0.25$, show how probability spreads out as $t \to \tau_s$. Recall that for a Brownian walker in three dimensions, there is an effective outward radial drift induced by the dimension of the walk. As a result, at $t = 0.15$ we see most of the probability move to the boundary, away from the target. Hence, τ_s is characterized by trajectories that initially travel away from the target and encounter the boundary, which directs the molecule around the domain to the target.

While this example is idealized, it illustrates how our asymptotic expansions can help understand the role of domain geometry in reaction-diffusion systems. One potential application is to cellular systems, where the shape of a cell or a membrane-enclosed region may influence the dynamics of cellular processes. The topic of how confinement effects first passage time properties has been explored in several recent studies [23, 24, 25, 26].

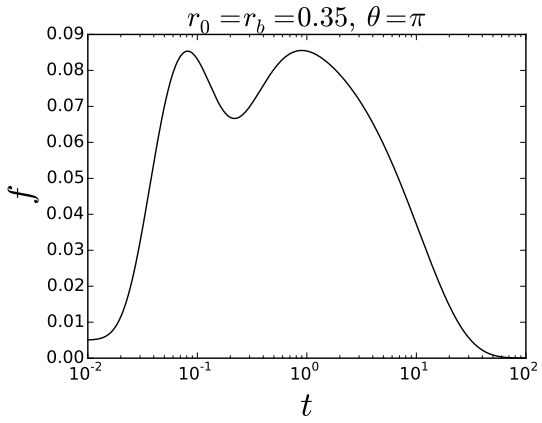

(a) The first passage time density.

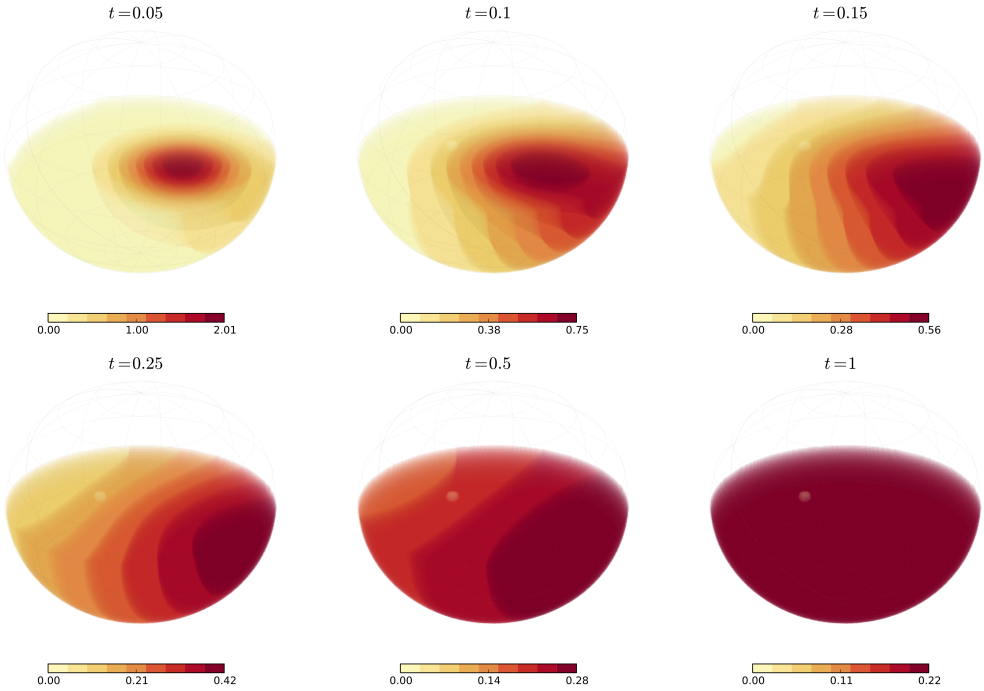

(b) The joint distribution function $p(\boldsymbol{r}, t)$.

Figure 4: The approximation for the (a) first passage time density $f(t)$ and (b) joint distribution $p(\boldsymbol{r}, t)$, where $\text{Prob}[\mathbf{R}(t) \in \mathcal{B}_{d\boldsymbol{r}}(\boldsymbol{r}), t < T] = p(\boldsymbol{r}, t)d\boldsymbol{r}$. The target radius is $\varepsilon = 0.03$. The target and initial position are placed along the center line $\theta_b = \pi$, $\theta_0 = 0$ at a distance of $r_b = r_0 = 0.35$.

4 Discussion

Including the occurrence of non-reactive encounters in bimolecular reaction models is a common and useful modeling tool for many complex biochemical reactions and cellular processes. Building upon our work on the pure-absorption reaction mechanism [1], we have developed comparable expansions for two partially-absorbing reaction mechanisms. Our approach extends the method of matched asymptotics as developed in [11] for estimating long-time asymptotic expansions, developing full uniform in time expansions of the solution to the underlying diffusion equation. This provides a versatile method that is complimentary to the pseudopotential approach we previously used for the pure absorption problem [1]. The approximations of the two partial reaction mechanisms differ by a single constant: the diffusion limited reaction rates given by (2.7) and (2.6).

The results presented here apply to general three-dimensional domains provided that the solution to the unperturbed problem is known. That is, to obtain the asymptotic approximation for a specific domain geometry, the primary necessary ingredient is the solution to (1.1) with no absorbing target (i.e., $\varepsilon = 0$). It is also of interest to obtain similar results for a Brownian search in two dimensions, since many biochemical reactions occur between membrane bound molecules [20, 27]. Unfortunately, in two-dimensions the asymptotic series contains $\frac{1}{\log \varepsilon}$ terms that converge slowly as $\varepsilon \to 0$. It may be possible to sum all of the logarithmic terms in the expansion and obtain an accurate approximation using methods similar to those in Ref. [28].

Another possible extension arises from observing that the matched asymptotic expansion method of [8, 11], which we used to derive the expansion of the large time component, does not require a spherical target. For non-spherical targets the inner problem is generally no longer exactly solvable, however, as described in [11] one can develop far-field expansions that are sufficient for matching inner and outer expansions. The inner solution behavior for different shapes, when "far" from the target, is accounted for by one parameter in the far-field expansions: the effective capacitance of the target object. It is an open problem to develop such expansions for the Doi reaction model with non-spherical targets, and it would be interesting to understand what differences the resulting Doi model expansions have from corresponding expansions of the solution to the Smoluchowski–Collins–Kimball model.

Many other extensions are possible given the breath of previous work on the large time approximation over the past few decades. If the domain contains multiple targets, splitting probabilities and conditional first passage times have been studied within the long time framework [29, 9]. The molecular motor mediated transport of viruses toward the cell nucleus is another example of a random target search problem, with added complexity that molecular motors move randomly with a directed bias toward the cell center [30]. We anticipate that as long as the probability flux around the target is approximately constant, our approximation framework should hold for search problems with drift.

Three dimensional search processes may also have active interactions with the domain boundary. The walker may be allowed to randomly stick to the domain boundary and diffuse along the 2D surface [31], as in a recent model of a T-cell searching for lymph nodes [32]. It is also

common for reactions to occur between molecules in the cytosol and membrane-bound proteins. In mathematical models these processes give rise to narrow escape problems [21, 9, 22]. The approximation obtained here breaks down as the target approaches the boundary, however, it is likely that a similar matched asymptotics procedure could be used to obtain uniform in time asymptotic expansions of solutions to the underlying diffusion equation for narrow escape problems.

5 Acknowledgments

SAI and AJM were partially supported by National Science Foundation awards DMS-0920886 and DMS-1255408. JMN was supported by a NSF-funded postdoctoral fellowship (NSF DMS-1100281, DMS-1462992). SAI and JMN would like to thank the Isaac Newton Institute for Mathematical Sciences, Cambridge, for support and hospitality during the programme on Stochastic Dynamical System in Biology, where work on this paper was undertaken. This work was supported by EPSRC grant no EP/K032208/1. SAI was also partially supported by a grant from the Simons Foundation to attend the programme as a visiting Simons Fellow.

A Finiteness of (2.42)

In this section we show

$$\lim_{\boldsymbol{r}\to\boldsymbol{r}_b}\left|\int_\Omega \tilde{G}(\boldsymbol{r},\boldsymbol{r}',s)p_0(\boldsymbol{r}')\,d\boldsymbol{r}'\right| < \infty, \quad \forall s>0, \tag{1.1}$$

where

$$p_0(\boldsymbol{r}) = \delta(\boldsymbol{r}-\boldsymbol{r}_0) - \frac{1}{|\Omega|} - \varepsilon w^{(1)}(\boldsymbol{r},\boldsymbol{r}_0) - \varepsilon^2 w^{(2)}(\boldsymbol{r},\boldsymbol{r}_0).$$

We show this identity holds for each order term in ε separately. At $O(1)$ we have

$$\int_\Omega \tilde{G}(\boldsymbol{r},\boldsymbol{r}',s)\left[\delta(\boldsymbol{r}-\boldsymbol{r}_0)-\frac{1}{|\Omega|}\right]d\boldsymbol{r}' = \tilde{G}(\boldsymbol{r},\boldsymbol{r}_0,s) - \frac{1}{s\,|\Omega|},$$

where we have used that

$$\begin{aligned}\int_\Omega \tilde{G}(\boldsymbol{r},\boldsymbol{r}',s)\,d\boldsymbol{r}' &= \int_0^\infty e^{-st}\left[\int_\Omega G(\boldsymbol{r},\boldsymbol{r}',t)\,d\boldsymbol{r}'\right]ds\\ &= \int_0^\infty e^{-st}\,ds,\\ &= \frac{1}{s}.\end{aligned}$$

Here the first line follows by the non-negativity of G and Fubini's theorem. As $s \to 0$ we have [1]

$$\lim_{s\to 0}\left(\tilde{G}(\boldsymbol{r},\boldsymbol{r}_0,s)-\frac{1}{s\,|\Omega|}\right)=U(\boldsymbol{r},\boldsymbol{r}_0).$$

We therefore conclude that for $\boldsymbol{r}_\mathrm{b}\neq\boldsymbol{r}_0$, the $O(1)$ contribution to (1.1) is bounded for each $s\geq 0$.

Recalling (2.27), at $O(\varepsilon)$ the behavior is determined by two integrals. The first is

$$U(\boldsymbol{r}_0,\boldsymbol{r}_\mathrm{b})\int_\Omega \tilde{G}(\boldsymbol{r},\boldsymbol{r}',s)\,d\boldsymbol{r}'=\frac{U(\boldsymbol{r}_0,\boldsymbol{r}_\mathrm{b})}{s},$$

which is clearly bounded for each $s>0$. The second is

$$\begin{aligned}\int_\Omega \tilde{G}(\boldsymbol{r},\boldsymbol{r}',s)U(\boldsymbol{r}',\boldsymbol{r}_\mathrm{b})\,d\boldsymbol{r}' &= \mathcal{L}\left[\int_t^\infty\left(G(\boldsymbol{r},\boldsymbol{r}',z)-\frac{1}{|\Omega|}\right)dz\right],\\ &= \frac{1}{s}\left[U(\boldsymbol{r},\boldsymbol{r}_\mathrm{b})-\tilde{G}(\boldsymbol{r},\boldsymbol{r}_\mathrm{b},s)+\frac{1}{s\,|\Omega|}\right], \qquad (1.2)\\ &= \frac{1}{s}\left[R_0(\boldsymbol{r},\boldsymbol{r}_\mathrm{b})-\left(\tilde{R}(\boldsymbol{r},\boldsymbol{r}_\mathrm{b},s)-\frac{1}{s\,|\Omega|}\right)+\frac{1-e^{-|\boldsymbol{r}-\boldsymbol{r}_\mathrm{b}|\sqrt{s/D}}}{\hat{k}_\mathrm{S}\,|\boldsymbol{r}-\boldsymbol{r}_\mathrm{b}|}\right], \qquad (1.3)\end{aligned}$$

where the identity in the first line is from [1]. For each fixed $s>0$, we see that the term in brackets is finite as $\boldsymbol{r}\to\boldsymbol{r}_\mathrm{b}$.

Finally, examining (2.28), at $O(\varepsilon^2)$ the only new term that appears is proportional to

$$\begin{aligned}&\int_\Omega \tilde{G}(\boldsymbol{r},\boldsymbol{r}',s)\left[\int_\Omega U(\boldsymbol{r}',\boldsymbol{r}'')U(\boldsymbol{r}'',\boldsymbol{r}_\mathrm{b})\,d\boldsymbol{r}''\right]d\boldsymbol{r}'\\ &\qquad=\frac{1}{s}\left[\int_\Omega U(\boldsymbol{r},\boldsymbol{r}'')U(\boldsymbol{r}'',\boldsymbol{r}_\mathrm{b})\,d\boldsymbol{r}''-\int_\Omega \tilde{G}(\boldsymbol{r},\boldsymbol{r}'',s)U(\boldsymbol{r}'',\boldsymbol{r}_\mathrm{b})\,d\boldsymbol{r}''\right],\end{aligned}$$

where we have switched the order of integration and used (1.2) (with $\boldsymbol{r}_\mathrm{b}$ replaced by $\boldsymbol{r}''$). Here changing the order of integration can be justified by expanding each term into their regular and singular parts to verify the integrand is absolutely integrable on the product space, and then applying Fubini's theorem. The second integral on the right hand side is finite as $\boldsymbol{r}\to\boldsymbol{r}_\mathrm{b}$ by (1.3). Moreover,

$$\int_\Omega U(\boldsymbol{r},\boldsymbol{r}')U(\boldsymbol{r}',\boldsymbol{r}_\mathrm{b})\,d\boldsymbol{r}'=\int_\Omega\left[\left(R_0(\boldsymbol{r},\boldsymbol{r}')+\frac{1}{\hat{k}_\mathrm{S}\,|\boldsymbol{r}-\boldsymbol{r}'|}\right)\left(R_0(\boldsymbol{r}',\boldsymbol{r}_\mathrm{b})+\frac{1}{\hat{k}_\mathrm{S}\,|\boldsymbol{r}'-\boldsymbol{r}_\mathrm{b}|}\right)\right]d\boldsymbol{r}'$$

can be seen to be finite as $\boldsymbol{r}\to\boldsymbol{r}_\mathrm{b}$ by changing to spherical coordinates about $\boldsymbol{r}_\mathrm{b}$ and noting the effective singularity within the integral is integrable (like $|\boldsymbol{r}-\boldsymbol{r}_\mathrm{b}|^{-2}$ as $\boldsymbol{r}\to\boldsymbol{r}_\mathrm{b}$).

B Proof of Lemma 2.1

Proof. For $0 \leq \varepsilon_1 \leq \varepsilon_2$ let

$$v(\boldsymbol{r}, t) = p_{\varepsilon_1}(\boldsymbol{r}, t) - p_{\varepsilon_2}(\boldsymbol{r}, t),$$

and denote by $\mathbb{1}_{\Omega_\varepsilon}(\boldsymbol{r})$ the indicator function on Ω_ε. Then

$$\frac{\partial v}{\partial t} = D\Delta v - \mu \mathbb{1}_{\Omega_{\varepsilon_1}}(\boldsymbol{r}) v + \mu \left[\mathbb{1}_{\Omega_{\varepsilon_2}}(\boldsymbol{r}) - \mathbb{1}_{\Omega_{\varepsilon_1}}(\boldsymbol{r})\right] p_{\varepsilon_2}(\boldsymbol{r}, t). \tag{2.1}$$

Let $G_\varepsilon(\boldsymbol{r}, \boldsymbol{r}', t)$ denote the Green's function solving

$$\begin{aligned}
\frac{\partial G_\varepsilon}{\partial t} &= D\Delta G_\varepsilon - \mu \mathbb{1}_{\Omega_\varepsilon}(\boldsymbol{r}) G_\varepsilon(\boldsymbol{r}, \boldsymbol{r}', t), \quad \boldsymbol{r} \in \Omega, t > 0, \\
\partial_{\boldsymbol{\eta}} G_\varepsilon(\boldsymbol{r}, \boldsymbol{r}', t) &= 0, \quad \boldsymbol{r} \in \partial\Omega, t > 0, \\
G_\varepsilon(\boldsymbol{r}, \boldsymbol{r}', 0) &= \delta(\boldsymbol{r} - \boldsymbol{r}'), \quad \boldsymbol{r} \in \Omega, \boldsymbol{r}' \in \Omega.
\end{aligned}$$

By Duhamel's Principle we may write

$$v(\boldsymbol{r}, t) = \int_0^t \int_\Omega G_{\varepsilon_1}(\boldsymbol{r}, \boldsymbol{r}', t - s) f(\boldsymbol{r}', s)\, d\boldsymbol{r}'\, ds,$$

where $f(\boldsymbol{r}', s)$ is given by

$$f(\boldsymbol{r}', s) := \mu \left[\mathbb{1}_{\Omega_{\varepsilon_2}}(\boldsymbol{r}') - \mathbb{1}_{\Omega_{\varepsilon_1}}(\boldsymbol{r}')\right] p_{\varepsilon_2}(\boldsymbol{r}', s),$$

and $f(\boldsymbol{r}', s) \geq 0$ as $\Omega_{\varepsilon_1} \subset \Omega_{\varepsilon_2}$. Since $G_{\varepsilon_1}(\boldsymbol{r}, \boldsymbol{r}', t) \geq 0$ we may conclude that

$$v(\boldsymbol{r}, t) \geq 0,$$

giving (2.53).

Finally, the inequality (2.54) is just a version of Theorem 2.3 of [17] adapted for Lipschitz domains, see Remark 3.11 of [17]. □

C Monte Carlo dynamic-lattice simulations

For comparison with the asymptotic expansions, we perform Monte Carlo simulations of the diffusion of a molecule to a spherical target at various locations within a spherical domain. The continuous motion of the diffusing molecule is approximated as a continuous-time random walk on lattice points. As will be described in more detail below, we allow the lattice to change dynamically to conform with the domain boundary or with the reactive boundary of the target. (The method used here is similar to the dynamic lattice version of the First-Passage Kinetic Monte Carlo (FPKMC) method in [33, 34]. However, here we do not use "protective domains" as are used in FPKMC, since there is only one diffusing molecule.)

The jump rate from a lattice point $\boldsymbol{x}_i$ to a neighboring lattice point $\boldsymbol{x}_j$ is given by D/h^2, where D is the diffusion coefficient and $h = |\boldsymbol{x}_i - \boldsymbol{x}_j|$ is the lattice spacing. This jump rate agrees with the standard second-order-accurate discretization of the Laplacian and has commonly been used in Reaction-Diffusion Master Equation (RDME) simulations as the jump rate between neighboring voxels [35, 36, 37].

Throughout the course of each simulation, the lattice is only defined locally. When the diffusing molecule is *not* near the target or the outer boundary of the domain, we set the lattice spacing equal to a specified value $h_1^{\max}$. Near the outer boundary of the domain, the local lattice spacing h will take on values less than or equal to $h_1^{\max}$ and is chosen in such a way as to enforce the reflecting boundary condition (described in more detail below). When the molecule is near the target, a finer lattice spacing is used. Specifically, when the distance from the diffusing molecule to the target is less than $2h_1^{\max}$, then the lattice spacing is chosen to be less than or equal to another specified value $h_2^{\max} \leq h_1^{\max}$. In Figures 2 and 3, $h_1^{\max} = 0.02$ and $h_2^{\max} = 0.005$.

Pure-absorption and Doi reaction mechanisms: First, we consider the cases of the Smoluchowski model with the pure-absorption Dirichlet reactive boundary or the Doi model. When the diffusing molecule is close enough to the target that a single hop of length $h_2^{\max}$ could take the molecule to within the target radius, then the local lattice spacing is chosen to be a value $h < h_2^{\max}$. This h is chosen so that a single hop may take the diffusing molecule exactly onto the target boundary, but not within the target (similar to Figure 3.3 and the left panel of Figure 3.4 in Ref. [34]). In the Dirichlet case, the simulation ends immediately when the diffusing molecule reaches the target boundary. In the Doi case, upon reaching the target boundary, a new local lattice of spacing $h_2^{\max}$ is defined. The molecule may then hop within the target or away from the target. When the distance from the diffusing molecule to the target center is less than or equal to the target radius, then the molecule may react with some probability per unit time given by the Doi reaction rate parameter. When the diffusing molecule is within the target, but has not yet reacted, and its distance to the target boundary is small enough that a single hop of length $h_2^{\max}$ could take the molecule outside the target, then the local lattice spacing is chosen to be a value $h < h_2^{\max}$ such that a single hop may take the diffusing molecule exactly onto the target boundary, but not outside the target. If the molecule hops to the target boundary, then the lattice spacing returns to $h_2^{\max}$, and the molecule may again hop either away from or into the target.

Partial-absorption reaction mechanism: In the case of the Smoluchowski–Collins–Kimball model with the partial-absorption Robin reactive boundary, a modified jump rate is used when the diffusing molecule is near the target. When the diffusing molecule is within a distance $h_2^{\max}/2$ from the target boundary, the lattice rotates to be perpendicular to the target boundary. The local lattice is defined so that the target boundary is exactly centered between two lattice points (similar to Figure 3.4, right panel, of Ref. [34]). The jump rate at the Robin boundary is $\dfrac{2D\gamma}{h(2D+\gamma h)}$, where γ is the Robin constant. We derived this jump rate following the approach in Appendix C of Ref. [38], but with their Dirichlet boundary condition replaced by a Robin boundary condition.

Outer domain boundary: The lattice also changes dynamically if the diffusing molecule is near the outer reflecting boundary of the overall simulation domain. Since the jump rate of D/h^2 gives

a coordinate-wise discretization, a different value of h can be used in each coordinate direction. The h in each coordinate will have a value less than or equal to $h_1^{\max}$, and is chosen so that the domain boundary lies exactly halfway between two lattice points (similar to Figure 3.5, right panel, of Ref. [34]). Then, the no-flux boundary condition is enforced by having a jump rate of zero across the boundary.

In Figs. 2 and 3, each subplot is based on $N = 10^5$ simulations for each of the three models. The histograms are obtained by binning the first passage time data from the simulations into intervals that are evenly spaced on a log scale. The error bars represent approximate 95% confidence intervals. Let Δt_i be the width of the i^{th} bin, N_i the number of observations in the i^{th} bin, and $p_i = N_i/N$. The error bars plotted at the center (on the log scale) of each bin are given by $p_i/\Delta t_i \pm 1.96\sqrt{(p_i)(1-p_i)}/(\sqrt{N}\Delta t_i)$.

References

[1] S. A. Isaacson and J. Newby, "Uniform asymptotic approximation of diffusion to a small target," *Phys Rev E*, vol. 88, no. 1, p. 012820 (13pp), 2013.

[2] M. Doi, "Second quantization representation for classical many-particle system," *J. Phys. A: Math. Gen.*, vol. 9, no. 9, pp. 1465–1477, 1976.

[3] ——, "Stochastic theory of diffusion-controlled reaction," *J. Phys. A: Math. Gen.*, vol. 9, no. 9, pp. 1479–1495, 1976.

[4] E. Teramoto and N. Shigesada, "Theory of bimolecular reaction processes in liquids," *Prog. Theor. Phys.*, vol. 37, no. 1, pp. 29–51, 1967.

[5] M. V. Smoluchowski, "Mathematical theory of the kinetics of the coagulation of colloidal solutions," *Z. Phys. Chem.*, vol. 92, pp. 129–168, 1917.

[6] F. C. Collins and G. Kimball, "Diffusion-controlled reaction rates," *J. Colloid. Sci.*, vol. 4, no. 4, pp. 425–437, 1949.

[7] T. Prüstel and M. Meier-Schellersheim, "The area reactivity model of geminate recombination," *J. Chem. Phys.*, vol. 140, no. 11, p. 114106, 2014.

[8] M. J. Ward and J. B. Keller, "Strong localized perturbations of eigenvalue problems," *SIAM J. Appl. Math*, vol. 53, no. 3, pp. 770–798, Jun 1993.

[9] A. F. Cheviakov, M. J. Ward, and R. Straube, "An asymptotic analysis of the mean first passage time for narrow escape problems: Part ii: The sphere," *Multiscale Model. Simul.*, vol. 8, no. 3, pp. 836–870, 2010.

[10] A. E. Lindsay, T. Kolokolnikov, and J. C. Tzou, "Narrow escape problem with a mixed trap and the effect of orientation," *Phys. Rev. E*, vol. 91, p. 032111, Mar 2015. [Online]. Available: http://link.aps.org/doi/10.1103/PhysRevE.91.032111

[11] A. F. Cheviakov and M. J. Ward, "Optimizing the principal eigenvalue of the Laplacian in a sphere with interior traps," *Mathematical and Computer Modelling*, vol. 53, no. 7-8, pp. 1394–1409, Apr. 2011.

[12] C. Chevalier, O. Bénichou, B. Meyer, and R. Voituriez, "First-passage quantities of Brownian motion in a bounded domain with multiple targets: a unified approach," *J. Phys. A-Math. and Theor.*, vol. 44, no. 2, p. 025002, Dec. 2010.

[13] J. Keizer, "Nonequilibrium statistical thermodynamics and the effect of diffusion on chemical reaction rates," *J. Phys. Chem.*, vol. 86, pp. 5052–5067, 1982.

[14] S. J. Chapman, R. Erban, and S. A. Isaacson, "Reactive boundary conditions as limits of interaction potentials for Brownian and Langevin Dynamics," 2015, arXiv:1507.03621 [physics.bio-ph].

[15] I. C. Agbanusi and S. A. Isaacson, "A comparison of bimolecular reaction models for stochastic reaction-diffusion systems," *Bull. Math. Biol.*, vol. 76, no. 4, pp. 922–946, 2013.

[16] R. Erban and S. J. Chapman, "Stochastic modelling of reaction-diffusion processes: algorithms for bimolecular reactions," *Phys. Biol.*, vol. 6, no. 4, p. 046001, Aug. 2009.

[17] R. F. Bass and P. Hsu, "Some potential theory for reflecting Brownian Motion in Hölder and Lipshitz domains," *The Annals of Probability*, vol. 19, no. 2, pp. 486–508, 1991.

[18] H. S. Carslaw and J. C. Jaeger, *Conduction of heat in solids*, 2nd ed. Oxford: Clarendon Press, 1959.

[19] A. D. Polyanin, *Handbook of Linear Partial Differential Equations for Engineers and Scientists*. Chapman & Hall/CRC, 2001.

[20] D. Holcman and Z. Schuss, "Escape through a small opening: Receptor trafficking in a synaptic membrane," *J. Stat. Phys.*, vol. 117, no. 5-6, pp. 975–1014, Dec 2004.

[21] Z. Schuss, A. Singer, and D. Holcman, "The narrow escape problem for diffusion in cellular microdomains," *PNAS*, vol. 104, no. 41, pp. 16 098–16 103, Oct 2007.

[22] S. Pillay, M. J. Ward, A. Peirce, and T. Kolokolnikov, "An asymptotic analysis of the mean first passage time for narrow escape problems: Part i: Two-dimensional domains," *Multiscale Model. Simul.*, vol. 8, no. 3, pp. 803–835, 2010.

[23] T. Guérin, N. Levernier, O. Bénichou, and R. Voituriez, "Mean first-passage times of non-markovian random walkers in confinement," *Nature*, vol. 534, no. 7607, pp. 356–359, 2016.

[24] T. G. Mattos, C. Mejía-Monasterio, R. Metzler, and G. Oshanin, "First passages in bounded domains: When is the mean first passage time meaningful?" *Phys. Rev. E*, vol. 86, p. 031143, Sep 2012.

[25] O. Bénichou, C. Chevalier, J. Klafter, B. Meyer, and R. Voituriez, "Geometry-controlled kinetics," *Nature chemistry*, vol. 2, no. 6, pp. 472–477, 2010.

[26] S. Condamin, O. Bénichou, V. Tejedor, R. Voituriez, and J. Klafter, "First-passage times in complex scale-invariant media," *Nature*, vol. 450, no. 7166, pp. 77–80, 2007.

[27] P. C. Bressloff, B. A. Earnshaw, and M. J. Ward, "Diffusion of protein receptors on a cylindrical dendritic membrane with partially absorbing traps," *SIAM J. Appl. Math.*, vol. 68, no. 5, pp. 1223–1246, 2007.

[28] M. Ward, W. Heshaw, and J. Keller, "Summing logarithmic expansions for singularly perturbed eigenvalue problems," *SIAM J. Appl. Math*, vol. 53, no. 3, pp. 799–828, Jun 1993.

[29] C. Chevalier, O. Bénichou, B. Meyer, and R. Voituriez, "First-passage quantities of brownian motion in a bounded domain with multiple targets: a unified approach," *Journal of Physics A: Mathematical and Theoretical*, vol. 44, no. 2, p. 025002, 2011.

[30] T. Lagache and D. Holcman, "Effective motion of a virus trafficking inside a biological cell," *SIAM J. Appl. Math.*, vol. 68, no. 4, pp. 1146–1167, 2007.

[31] O. Bénichou, D. Grebenkov, P. Levitz, C. Loverdo, and R. Voituriez, "Optimal reaction time for surface-mediated diffusion," *Physical review letters*, vol. 105, no. 15, p. 150606, 2010.

[32] M. I. Delgado, M. J. Ward, and D. Coombs, "Conditional mean first passage times to small traps in a 3-d domain with a sticky boundary: Applications to t cell searching behavior in lymph nodes," *Multiscale Modeling & Simulation*, vol. 13, no. 4, pp. 1224–1258, 2015.

[33] A. J. Mauro, J. K. Sigurdsson, J. Shrake, P. J. Atzberger, and S. A. Isaacson, "A first-passage kinetic Monte Carlo method for reaction-drift-diffusion processes," *J. Comp. Phys.*, vol. 259, pp. 536–567, 2014.

[34] A. J. Mauro, "Numerical methods and stochastic simulation algorithms for reaction-drift-diffusion systems," Ph.D. dissertation, Boston University, 2014, available at http://search.proquest.com/docview/1629025381. [Online]. Available: http://search.proquest.com/docview/1629025381

[35] S. A. Isaacson and C. S. Peskin, "Incorporating diffusion in complex geometries into stochastic chemical kinetics simulations," *SIAM J. Sci. Comput.*, vol. 28, no. 1, pp. 47–74, 2006.

[36] S. A. Isaacson, D. M. McQueen, and C. S. Peskin, "The influence of volume exclusion by chromatin on the time required to find specific DNA binding sites by diffusion," *PNAS*, vol. 108, no. 9, pp. 3815–3820, Mar. 2011.

[37] S. A. Isaacson, C. A. Larabell, M. A. Le Gros, D. M. McQueen, and C. S. Peskin, "The influence of spatial variation in chromatin density determined by X-ray tomograms on the time to find DNA binding sites," *Bull. Math. Bio.*, vol. 75, no. 11, 2013.

[38] H. Wang, C. S. Peskin, and T. C. Elston, "A robust numerical algorithm for studying biomolecular transport processes," *J. Theor. Biol.*, vol. 221, pp. 491–511, 2003.